Changes in neuronal genes in prenatally alcohol-exposed placentas correlate with neuropsychological traits at the age of six

Rämö K[1], Wallén E[1], Saure E[2], Jolma M[3], Auvinen P[1], Kahila H[4], Kaminen-Ahola N[1*]

1. Environmental Epigenetics Laboratory, Department of Medical and Clinical Genetics, Medicum, University of Helsinki, Helsinki, Finland

2. BABA Center, Pediatric Research Center, Helsinki University Hospital and University of Helsinki, Helsinki, Finland

3. Division of Child Neurology, Päijät-Häme Central Hospital, Lahti, Finland, and Faculty of Medicine, University of Helsinki, Helsinki, Finland

4. Department of Obstetrics and Gynecology, Helsinki University Hospital and University of Helsinki, Helsinki, Finland

*Corresponding author

ABSTRACT

Prenatal alcohol exposure (PAE) disrupts embryonic development and gives rise to a variable fetal alcohol spectrum disorder (FASD) phenotype characterized by neurodevelopmental and dysmorphological defects. We investigated the effects of PAE on placental gene regulation by performing genome-wide DNA methylation (DNAm) microarray and gene expression (mRNA sequencing) analyses in 87 PAE, 77 unexposed control, and 11 smoking-exposed-only placentas. Significant alterations were identified in genes involved in synaptic function including both excitatory and inhibitory neurotransmission, and in genes previously associated with attention-deficit/hyperactivity disorder (ADHD), autism spectrum disorder, schizophrenia, and addiction. When placental molecular alterations were compared with neuropsychological and dysmorphological phenotypes of the same children assessed at six years of age, numerous correlations were observed between DNAm and gene expression, as well as head circumference, cognitive performances, ADHD traits, and dysmorphology. These included associations between *DAOA* methylation and verbal intellectual abilities and language development, *GPHN* methylation and working memory index, and *GLI3* expression

and both working memory index and midfacial hypoplasia. As these alterations were observed in the placenta, this tissue not only enables the identification of phenotype-specific FASD candidate genes but also represents a valuable tool for studying complex developmental disorders in human.

INTRODUCTION

The intrauterine environment has an impact on the development and lifelong health of the individual. Prenatal alcohol exposure (PAE) is one of the most harmful environmental factors and a major public health concern globally[1]. PAE has been associated with a variety of developmental disorders including central nervous system (CNS) dysfunction, craniofacial malformations, and growth restriction[2], which fall under the umbrella term of fetal alcohol spectrum disorders (FASD). The features of complex FASD phenotype overlap with other neurodevelopmental disorders (NDD), such as attention-deficit/hyperactivity disorder (ADHD) and autism spectrum disorder (ASD), as well as with schizophrenia (SCZ)[3,4], which has a strong neurodevelopmental component[5]. PAE significantly increases the risk of mental health disorders such as depression, anxiety as well as learning and memory deficits[6] and addiction[7].

The developing nervous system is particularly sensitive to the effects of PAE[8,9]. Several *in vitro* models and animal studies have shown that early alcohol exposure can alter epigenetic marks, such as DNA methylation (DNAm), affect gene regulation, and disrupt embryonic developmental programming[10]. The DNAm and gene expression of gastrulating ectodermal cells are particularly sensitive to *in vitro* alcohol exposure[9] and PAE in a mouse model, corresponding developmentally to the first four weeks of human pregnancy, can induce changes in the offspring's DNAm and lead to long-lasting effects on gene expression and phenotype [11,12]. Indeed, alcohol-related neurodevelopmental disorders (ARNDs) constitute the most common subgroup of FASD[13]. It has been shown that alcohol disrupts synaptic function and plasticity subsequently affecting the formation and remodeling of neuronal networks[14]. Consistent with this, in a PAE mouse model, altered synaptic and mitochondrial gene expression and imbalance of excitatory/inhibitory (E/I) synaptic activity in the brain as well as cognitive and behavioral abnormalities have been observed[15]. During prenatal development, these alterations have been associated with CNS structural anomalies[16],

neurocognitive deficits, and behavioral disorders such as hyperactivity, anxiety-like-behaviour, and impairment of memory and learning[17].

The placenta is a temporary organ that not only transfers nutrients, oxygen, and antibodies from the maternal circulation to the fetus but also produces hormones, such as growth hormones and neuropeptides, and acts as a partial barrier against harmful substances[18]. It is an easily accessible tissue, and recent studies have suggested that it could be a useful tissue to investigate the effects of the intrauterine environment on human development – also on neurodevelopment. Differentially methylated regions (DMRs) in the placenta have been shown to be enriched in genes involved in neuronal development and synaptic function[19–21]. Also, similar NDD-associated DNAm profiles and gene expression have been observed in both placenta and brain tissues in mouse[22] and human[21]. Some associations between placental DNAm and later neurodevelopmental outcomes such as cognitive functions and ASD in human have been detected[23,24]. Therefore, the placenta can provide molecular insights into the fetal origins of NDDs, as well as reveal epigenetic markers that may serve as early indicators of neurodevelopmental risks. The mechanisms that underlie the observed associations remain obscure, but recent findings have heightened interest in the poorly understood placenta–brain axis[25] and neuroplacentology[26].

To explore the molecular etiology of FASD, we have collected placental samples from prenatally alcohol- and smoking-exposed as well as control newborns. We have focused on the effects of PAE on the methylome and transcriptome of placenta and excluded the impact of smoking, a common confounding factor, by adding smoking-exposed-only placentas (SEO) to the control group. Furthermore, the observed PAE-associated alterations were confirmed by excluding all smoking-exposed placentas and comparing a subgroup of only alcohol-exposed placentas to the controls. To explore potential links between the observed PAE-associated molecular alterations in the placenta and phenotypes, we have performed neuropsychological and dysmorphological assessments on the same children at the age of six[27]. The majority (76%) of the PAE children met the criteria of FASD at this age. Finally, we performed correlation analyses between the DNAm and expression of placental PAE-associated genes and head circumference (HC) as well as cognitive, ADHD, FAS dysmorphology, and midfacial hypoplasia traits of the children.

RESULTS

Characteristics of the cohort

General characteristics of 87 (41 males and 46 females) PAE and 88 control (including 77 unexposed: 42 males and 35 females, and 11 SEO: 3 males and 8 females) newborns as well as their mothers were compared (Supplementary Table S1). PAE newborns had significantly lower gestational age (P=0.001, Mann-Whitney U), lower birth weight (SD) (P=0.043, Student's t-test), and smaller HC (standard deviation, SD) (P=0.02, Student's t-test) compared to controls and smoking-exposed newborns. Without smoking-exposed samples, the PAE newborns still had significantly smaller HC (SD) (P=0.035, Student's t-test).

Mothers of PAE newborns had significantly higher pre-pregnancy BMI (P=0.017, Mann-Whitney U) and lower gestational weight gain (P=0.015, Student's t-test) compared to control mothers. Also, all smoking-exposed samples were excluded and 16 only PAE and 77 unexposed control newborns as well as their mothers were compared (Supplementary Table S1). The mothers of only PAE newborns still had higher pre-pregnancy BMI (P<0.001, Mann-Whitney U).

PAE-associated genome-wide DNAm in placenta

The effects of PAE on placental genome-wide DNAm were studied by microarrays (EPIC, Illumina) for 87 PAE and 88 control (including 77 unexposed and 11 SEO) placental samples. The analysis resulted in 3862 significantly differentially methylated CpG sites (53% hypomethylated) with FDR < 0.05 (Figure 1a, Supplementary Table S2). To separate the most prominent changes and minimize false positive hits due to the observed inflation, we focused on the CpG sites with DNAm difference in the effect size of ≥5% between PAE and control placentas, which were termed as differentially methylated positions (DMPs). We observed 225 PAE associating DMPs (22% hypomethylated) linking to 154 genes (FDR < 0.05, $\Delta\beta \leq -0.05$ and $\Delta\beta \geq 0.05$).

Several PAE-associated hypomethylated DMPs linked to *CCR6, TRIM5* and *SLC12A8*, and hypermethylated to *DAPK1, ERICH1, ARHGEF10, DAOA, CTBP2, TSNARE1, GTDC1,* and *GPHN* (Figure 1a). The most hypomethylated DMPs linked to *CCR6* (*Chemokine receptor 6*), a key player in immune responses involving inflammation[28]. The most hypermethylated DMPs associated with *DAPK1 (Death-associated protein kinase 1*), a mediator of gamma-

interferon induced programmed cell death and *ERICH1 (Glutamate-Rich 1).* The highest number of hypermethylated DMPs associated with *ARHGEF10 (Rho guanine nucleotide exchange factor 10),* which regulates the activity of small Rho GTPases, proteins crucial for neuronal shape, polarity, migration, and connectivity during brain development[29].

Also, DMRs, defined as a region with maximal allowed genomic distance of 1000 bp containing three or more CpGs with $P < 0.05$ according to Fisher's combined probability test, were analyzed. A total of 506 placental DMRs associated with PAE were revealed (Supplementary Table S3). The most significant hypomethylated DMRs associated with *CCR6, TNXB, TILL1, GDF2, ZHX2, GSDMD, GUCY1B2, TMEM216, HECW1, GTSF1, ZIC1, CD52, TTC32, PPP1R18, PCCA,* and *HOXC6,* as well as imprinted *FAM50B* and *PEG10.* Hypermethylated DMRs associated with *ESRRG, TSNARE1, SATB2, HLA-F, FRZB, SLC6A12,* and *ARHGEF10*. A total of three hypermethylated DMRs were associated with *TSNARE1(t-SNARE domain containing 1),* which primarily acts as a regulator of endosomal trafficking in neurons, especially in the brain[30].

According to the Gene Ontology (GO) pathway analysis, the observed alterations in placental DNAm were enriched most significantly in terms such as membrane repolarization during ventricular cardiac muscle cell action potential, negative regulation of fat cell proliferation, cell junction organization, and postsynaptic density assembly ($P<0.05$) (Figure 1b, Supplementary Table S4). PAE-associated alterations in DMRs enriched in terms such as skeletal system development, negative regulation of neuron differentiation, cartilage development, as well as cochlea and inner ear morphogenesis ($P<0.05$) (Figure 1c, Supplementary Table S5). All these processes have been previously associated with FASD phenotype [2,31].

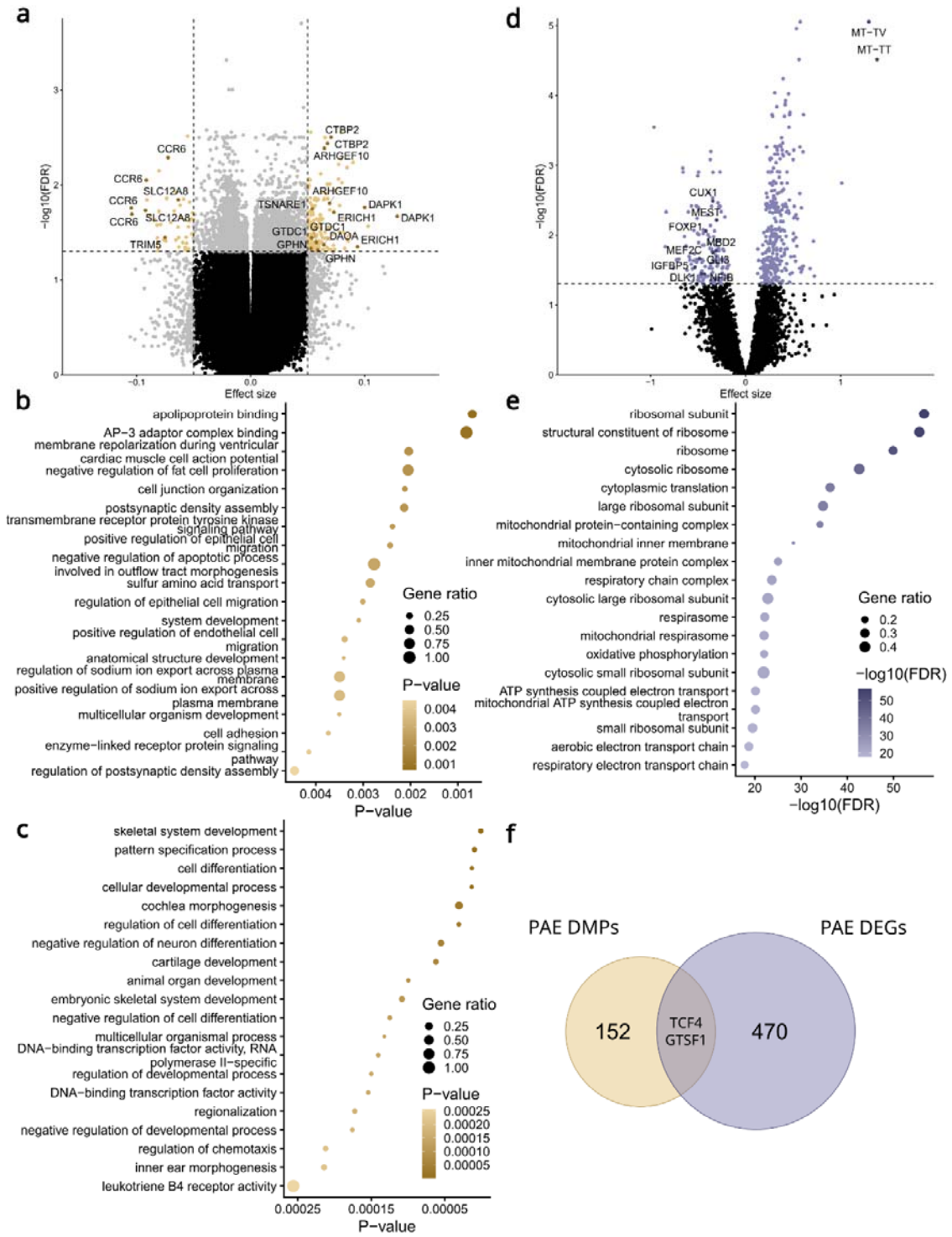

Figure 1. PAE-associated differential DNAm, gene expression, and canonical pathways in the placenta. **a)** Volcano plot showing the distribution of associations between placental CpG sites and PAE. Horizontal line marks FDR 0.05 and vertical line marks effect size ± 0.05. Enriched terms identified in GO pathway analysis of PAE-associated **b**) differentially methylated CpGs (FDR<0.05) and **c)** DMRs in the placenta. In pathway analyses, the 20

most significant pathways are shown. **d)** Volcano plot showing the distribution of associations between mRNA expression and PAE. Horizontal line marks FDR 0.05. **e)** Enriched terms identified in GO pathway analysis of PAE-associated DEGs (FDR < 0.05) in the placenta. **f)** Venn diagram showing the number of PAE-associated DMPs, DEGs, and the common genes.

PAE-associated mRNA expression in placenta

To explore PAE-associated gene expression, we performed mRNA-seq for 61 PAE and 48 control (including 41 unexposed and 7 SEO) placental samples. We observed 472 significantly differentially expressed genes (DEGs) (FDR < 0.05) of which 68% were upregulated (Figure 1b, Supplementary Table S6). The most upregulated genes were MT-TT and MT-TV, which encode mitochondrial tRNA molecules for threonine and valine, respectively. According to the GO enrichment analysis, PAE-associated gene expression is linked predominantly to ribosomes as well as mitochondrial protein-containing complex, inner membrane, and respiratory chain complex (FDR<0.05, Figure 1e, Supplementary Table S7). According to the MitoXplorer database[32], 19% of DEGs associated with mitochondrial functions, mainly with oxidative phosphorylation, translation, and reactive oxygen species defence (Supplementary Table S8). There were only two overlapping genes between DEGs and genes associated with DMPs (Fig. 1f).

Sensitivity tests for DNAm and gene expression analyses

To confirm the PAE-specificity of the observed alterations, we performed genome-wide DNAm analysis for 16 only alcohol-exposed PAE and 77 control, and mRNA-seq analysis for 10 PAE and 41 control placentas, all groups without smoking-exposed samples. In the DNAm analysis, we observed 108 significantly differentially methylated CpG sites with FDR < 0.05, of which 30% were hypomethylated (Supplementary Figure S1, Supplementary Table S9). A total of five genes were involved in synaptic function according to the SynGO database[33](Supplementary Table S10). The highest number of PAE-associated hypermethylated probes were linked to *GPHN* (gephyrin), a protein involved in the postsynaptic clustering of GABA alpha and glycine receptors[34]. The most hypomethylated DMP associated with a neurokinin B signaling mediator *TACR3* (*tachyrin receptor 3)*, which was also the most hypomethylated gene in our previous study, in which SEO placentas were not included in the controls[19].

In the gene expression sensitivity analysis, we observed 295 DEGs (FDR < 0.05) of which 77% were upregulated (Supplementary Figure S1, Supplementary Table S11). Consistently with the main mRNA-seq analysis, PAE-associated alterations were enriched most significantly with ribosomes and mitochondrial functions (Supplementary Table S7), and also approximately 50% of the previously observed synapse-specific DEGs were detected in this comparison, such as upregulated *GABARAP* (*GABA type A receptor-associated protein).*

PAE-associated alterations in neurodevelopmental genes

In addition to several developmentally essential PAE-associated genes, such as hypermethylated *NODAL*, *MNX1*, and *HOXA1*, as well as downregulated *IGFBP5*, *DLK1*, *MEF2C*, *NFIB*, *FOXP1*, *CUX1*, *GLI3*, *MBD2*, and *MEST*, we observed numerous genes involved in synaptic function according to the SynGO database[33]. DMPs, mainly hypermethylated, associated with 18 synaptic genes (Table 1a). The only hypomethylated DMPs were in postsynaptic *GRIN3A* (*Glutamate NMDA receptor subunit 3A*) and *NRN1 (Neuritin 1)*, which associated with presynaptic modulation of chemical synaptic transmission. Moreover, a total of 73 synapse-associated DEGs, including 42 upregulated ribosomal genes (Supplementary Table S10) and 31other genes (48% upregulated), were observed (Table 1b).

Furthermore, in this study, 52 (8.3%) of PAE-associated genes overlapped with ADHD genes[35], 49 (7.6%) with ASD[36], and 218 (34.9%) with schizophrenia[37] (Figure 2, Supplementary Table S12). Additionally, many of the altered genes, such as *ARHGEF10*[38], *DLGAP2*[39], *FOS*[40], *GATA4*[41], *GPHN*[42], *GRIN3A*[43], and *TACR3*[44] have also been previously associated with alcohol addiction or dependence.

Table 1. Synaptic genes, which linked to PAE-associated alterations in DNAm (DMPs) and gene expression (DEGs) in the placenta. Genes, their cellular component locations, and involved biological processes based on **a)** DNAm analysis and **b)** mRNA sequencing analysis according to SynGO database. DMP-associated CpGs (FDR < 0.05) have also been reported.

a)

Gene	Gene name	Location based on Cellular Component GO terms	Function based on Biological Process GO terms	PAE-associated DMPs

ATP2B2	ATPase plasma membrane Ca2+ transporting 2	integral component of postsynaptic density membrane (GO:0099061), integral component of postsynaptic membrane (GO:0099055)	ATPase-coupled calcium ion transmembrane transporter activity involved in regulation of postsynaptic cytosolic calcium levels (GO:1905059)	hypermethylated DMP (body) + 7 CpGs (TSS200, 3'UTR, 5'UTR, body)
CACNG7	calcium voltage-gated channel auxiliary subunit gamma 7	integral component of postsynaptic density membrane (GO:0099061)	neurotransmitter receptor localization to postsynaptic specialization membrane (GO:0099645), regulation of postsynaptic neurotransmitter receptor activity (GO:0098962)	hypermethylated DMP + CpG (TSS1500)
CCK	cholecystokinin	neuronal dense core vesicle lumen (GO:0099013)	synaptic signaling via neuropeptide (GO:0099538)	hypermethylated DMP (body)
CDH1	cadherin 1	postsynapse (GO:0098794)	regulation of protein catabolic process at postsynapse, modulating synaptic transmission (GO:0099576)	hypermethylated DMP (body)
CRMP1	collapsin response mediator protein 1	presynapse (GO:0098793), postsynapse (GO:0098794)	regulation of postsynapse assembly (GO:0150052)	hypermethylated DMP (body)
CTBP2	C-terminal binding protein 2	presynaptic cytosol (GO:0099523)	structural constituent of active zone (GO:0098882), synaptic vesicle docking (GO:0016081)	2 hypermethylated DMPs (5'UTR)
DAPK1	death associated protein kinase 1	postsynaptic density (GO:0014069)		3 hypermethylated DMPs (body)
DGKQ	diacylglycerol kinase theta	presynapse (GO:0098793), postsynapse (GO:0098794)	regulation of synaptic vesicle endocytosis (GO:1900242)	hypermethylated DMP (body) + 2 CpGs (body, 3'UTR, TSS1500)
DLGAP2	DLG associated protein 2	postsynaptic density, intracellular component (GO:0099092)	regulation of postsynaptic neurotransmitter receptor activity (GO:0098962),	hypermethylated DMP (body) + 2 CpGs (body,

			modulation of chemical synaptic transmission (GO:0050804)	TSS200)
GPC6	glypican 6	synapse (GO:0045202)	regulation of neurotransmitter receptor localization to postsynaptic specialization membrane (GO:0098696)	hypermethylated DMP (body)
GPHN	gephyrin	postsynaptic specialization, intracellular component (GO:0099091)	neurotransmitter receptor localization to postsynaptic specialization membrane (GO:0099645)	2 hypermethylated DMPs (body) + 2 CpGs (TSS1500, 3'UTR)
GRIN3A	glutamate ionotropic receptor NMDA type subunit 3A	integral component of postsynaptic density membrane (GO:0099061)	presynaptic modulation of chemical synaptic transmission (GO:0099171), transmitter-gated ion channel activity involved in regulation of postsynaptic membrane potential (GO:1904315)	hypomethylated DMP (TSS200) + CpG (TSS200)
NCAM2	neural cell adhesion molecule 2	integral component of synaptic membrane (GO:0099699)		hypermethylated DMP (TSS1500)
NRN1	neuritin 1	postsynaptic endocytic zone (GO:0098843)	presynaptic modulation of chemical synaptic transmission (GO:0099171), regulation of synapse maturation (GO:0090128), transport	hypomethylated DMP (body)
NTM	neurotrimin	anchored component of postsynaptic density membrane (GO:0099031), presynaptic active zone membrane (GO:0099029)		hypermethylated DMP (body)
PRKN	parkin RBR E3 ubiquitin protein ligase	postsynapse (GO:0098794), presynapse (GO:0098793), synaptic vesicle membrane	regulation of postsynaptic membrane neurotransmitter receptor levels (GO:0099072), regulation protein catabolic process at presynapse	hypermethylated DMP (body)

		(GO:0030672)	(GO:0140251), regulation of synaptic vesicle endocytosis (GO:1900242)	
PTPRD	protein tyrosine phosphatase receptor type D	integral component of presynaptic membrane (GO:0099056)	modulation of chemical synaptic transmission (GO:0050804), trans-synaptic signaling (GO:0099537), synapse adhesion between pre- and post-synapse (GO:0099560)	hypermethylated DMP (body)
WASF3	WASP family member 3	postsynapse (GO:0098794)	modification of postsynaptic actin cytoskeleton (GO:0098885)	hypermethylated DMP (5'UTR)

b)

Gene	**Gene name**	**Location based on Cellular Component GO terms**	**Function based on Biological Process GO terms**	**PAE-associated DEGs**
AAK1	AP2 associated kinase 1	presynapse (GO:0098793)	presynaptic endocytosis (GO:0140238)	downregulated
ABI2	abl interactor 2	postsynaptic actin cytoskeleton (GO:0098871)	postsynaptic actin cytoskeleton organization (GO:0098974), presynaptic actin cytoskeleton organization (GO:0099140), synaptic vesicle clustering (GO:0097091)	downregulated
ABL2	ABL proto-oncogene 2, non-receptor tyrosine kinase	postsynapse (GO:0098794)	synapse maturation (GO:0060074)	downregulated
AP1B1	adaptor related protein complex 1 subunit beta 1	synaptic vesicle (GO:0008021)		downregulated
ARPC2	actin related protein 2/3 complex subunit 2	presynapse (GO:0098793), postsynapse (GO:0098794), synapse (GO:0045202), synaptic vesicle membrane (GO:0030672)		upregulated
ARPC3	actin related protein 2/3		regulation of synaptic vesicle endocytosis (GO:1900242)	upregulated

	complex subunit 3			
ATP6V1F	ATPase H+ transporting V1 subunit F	extrinsic component of synaptic vesicle membrane (GO:0098850)	synaptic vesicle proton loading (GO:0097401)	upregulated
CLTA	clathrin light chain A	synaptic vesicle membrane (GO:0030672), presynaptic endocytic zone membrane (GO:0098835)	synaptic vesicle endocytosis (GO:0048488)	upregulated
CLU	clusterin	synapse (GO:0045202)		upregulated
CRIPT	CXXC repeat containing interactor of PDZ3 domain	postsynaptic density, intracellular component (GO:0099092)	regulation of postsynaptic density assembly (GO:0099151)	upregulated
CYFIP1	cytoplasmic FMR1 interacting protein 1	postsynapse (GO:0098794)	regulation of translation at postsynapse, modulating synaptic transmission (GO:0099578), regulation of modification of postsynaptic actin cytoskeleton (GO:1905274)	downregulated
EEF1D	eukaryotic translation elongation factor 1 delta	synapse (GO:0045202)		upregulated
EIF3B	eukaryotic translation initiation factor 3 subunit B	synapse (GO:0045202)		downregulated
GABARAP	GABA type A receptor-associated protein	postsynaptic specialization, intracellular component (GO:0099091)	regulation of neurotransmitter receptor localization to postsynaptic specialization membrane (GO:0098696)	upregulated
ITGB4	integrin subunit beta 4	integral component of postsynaptic membrane (GO:0099055)		downregulated
LAMA4	laminin subunit alpha 4	synaptic cleft (GO:0043083)		downregulated
LAMB2	laminin subunit	synaptic cleft (GO:0043083)	structural constituent of synapse-	downregulated

	beta 2		associated extracellular matrix (GO:0150043)	
LAMC1	laminin subunit gamma 1	synaptic cleft (GO:0043083)		downregulated
LRP1	LDL receptor related protein 1	integral component of postsynaptic density membrane (GO:0099061)	regulation of postsynaptic neurotransmitter receptor endocytosis (GO:0099149)	downregulated
NUDT3	nudix hydrolase 3	synapse (GO:0045202)		downregulated
PLS3	plastin 3		regulation of synaptic vesicle cycle (GO:0098693), structural constituent of presynaptic actin cytoskeleton (GO:0098699)	downregulated
PNKD	PNKD metallo-beta-lactamase domain containing	presynaptic cytosol (GO:0099523)		upregulated
PPP1CA	protein phosphatase 1 catalytic subunit alpha	presynapse (GO:0098793), postsynapse (GO:0098794)		upregulated
PSENEN	presenilin enhancer, gamma-secretase subunit	integral component of presynaptic membrane (GO:0099056)		upregulated
ROCK1	Rho associated coiled-coil containing protein kinase 1	synapse (GO:0045202)	regulation of synapse maturation (GO:0090128)	downregulated
SNAP29	synaptosome associated protein 29	synaptic vesicle (GO:0008021), extrinsic component of synaptic vesicle membrane (GO:0098850)	regulation of synaptic vesicle cycle (GO:0098693), regulation of synaptic vesicle exocytosis (GO:2000300)	upregulated
SNAPIN	SNAP	presynapse (GO:0098793),	regulation of synaptic vesicle exocytosis	upregulated

	associated protein	synaptic vesicle (GO:0008021)	(GO:2000300)	
TIAM1	TIAM Rac1 associated GEF 1	extrinsic component of postsynaptic density membrane (GO:0099147)	regulation of postsynapse organization (GO:0099175), regulation of modification of postsynaptic actin cytoskeleton (GO:1905274)	downregulated
VAPA	VAMP associated protein A	integral component of presynaptic membrane (GO:0099056), presynaptic cytoskeleton (GO:0099569)		upregulated
VPS11	VPS11 core subunit of CORVET and HOPS complexes	presynaptic active zone (GO:0048786)		downregulated
VPS29	VPS29 retromer complex component		regulation of synaptic vesicle endocytosis (GO:1900242)	upregulated

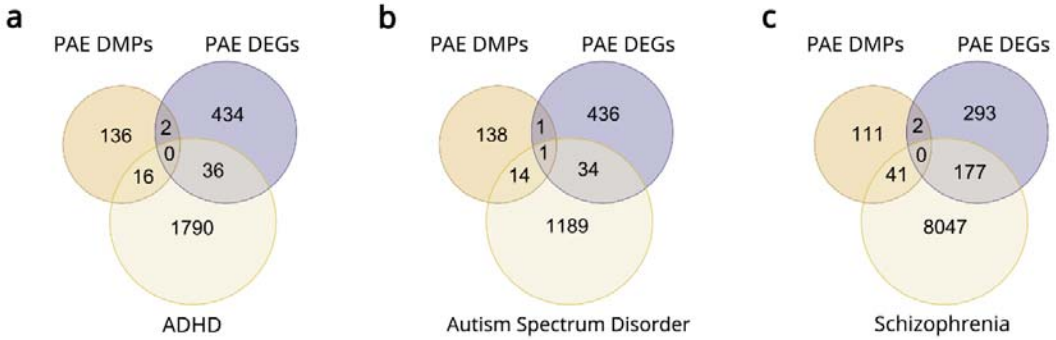

Figure 2. Common genes between PAE-associated DNAm and gene expression, and NDDs with overlapping phenotypes. PAE associated DMPs and DEGs were compared to **a)** ADHD, **b)** autism spectrum disorder, and **c)** schizophrenia genes (Hongyao et al. 2023, SFARI, and SZDB, respectively).

Placental DNAm and gene expression correlated with children's phenotype

Neuropsychological and dysmorphological assessments for 28 PAE and 52 unexposed control children have been performed at the age of six[27]. Smaller HCs, lower cognitive performance scores, higher prevalence of ADHD symptoms, and dysmorphological features such as midfacial hypoplasia were significantly associated with the PAE children. To explore potential correlations between molecular alterations in the placenta and phenotypic features, we performed correlation analyses between DMPs and DEGs, and HCs (SD) as well as cognitive, ADHD Rating Scale (ADHD-RS), FAS dysmorphology, and midfacial hypoplasia scores. DMPs and DEGs from both main and sensitivity analyses, and in addition to DMPs also differentially methylated CpGs associating with same genes (FDR<0.05), were used in the correlation analyses. Several, mainly moderate correlations with nominally significant *P*-values (*P*<0.01 or *P*<0.05) were observed (Supplementary Table S13). Also, correlations between DNAm, gene expression, and maternal alcohol consumption according to AUDIT scores and alcohol doses were examined (Table 2, Supplementary Table S13). Among correlated genes, *APOC1*[45], *CYTL1*[46], *GLI3*[47], *GPHN*[42], *GSDMD*[48], *JAG1*[49], *NUDT3*[50], *RBM25*[51], *SMARCA4*[52], *S100A6*[53], *VWF*[54], and *ZFAND2A*[55], have all been associated with alcohol exposure in previous studies (*P*<0.05, Spearman).

Table 2. Correlations between placental PAE-associated genes and maternal alcohol consumption. Significant correlations in DNAm and gene expression with nominal *P*-values <0.05 are shown in the table (Spearman). Genes previously associated with alcohol exposure are shown in bold.

AUDIT scores		Alcohol doses	
DNAm (*n* = 54)	*CACNG7, CCR6, DUXA,* ***GPHN****, NR2F1_MIR548AO, NTM, PLEKHM3, TRIM5, TSNARE1, WASF3* Only PAE: ***GPHN***	**DNAm** (*n* = 28)	*ARHGEF10, DHRS2,* ***GSDMD****, KIAA0649, RPSAP58, SULF1, TSNARE1, ZNF516*
mRNA (*n* = 33)	*ANKRD11,* ***APOC1****, BAZ2A, CDH5, CLU, COA5, COX14, CTSO, ENPEP, FAM160B2,* ***GLI3****, GLRX3, H1-2, H2AC6, INO80C,* ***JAG1****, LAMTOR4, NFIB,* ***NUDT3****, OST4,* ***S100A6****, SDHB, SERP1, SPCS1, TMEM59, TRIM44,* ***ZFAND2A*** Only PAE: *MTHFS,* ***RBM25****, UPF3A*	**mRNA** (*n* = 21)	***CYTL1****, MRPL52, NEK7, RPS29, SBDSP1, SLC12A9,* ***SMARCA4****, TMEM127,* ***VWF****,* ***ZFAND2A*** Only PAE: *UBE2Q2*

PAE-associated placental alterations correlated with HC at birth and at the age of six

Since HC is commonly used as an indirect marker of early brain development[56], we first analyzed correlations between DNAm, gene expression and HC (SD) at birth and at the age of six. At birth, DNAm of several genes correlated with HC (SD), among which *CAMTA1*[57], *GRIN3A*[58], *HOXA1*[59], *MYT1L*[60], *NR2F1*[61], *PARK2*[62], *PRDM16*[63], *PTPRD*[64], and *RAI1*[65] have all been associated with HC and/or brain growth in previous studies ($P<0.05$, Spearman) (Table 3, Supplementary Table S13). Also, a high number of correlations were observed between gene expression and HC (SD), of which *BCAP31*[66], *KMT2C*[67], *POGZ*[68], and *RPS6*[69] ($P<0.05$, Spearman) have previously been linked with HC and/or brain growth.

At six years of age, DNAm of *GTDC1* and *GATA4* correlated most significantly with HC (SD) (r=-0.356, P=0.002 and r=-0.302, P=0.009, respectively, Spearman) (Table 3, Supplementary Table S14). Among all correlating genes, *GTDC1*[70], *NCAM2*[71], and *NR2F1*[61] have been associated with HC and/or brain growth in previous studies. Moreover, among the correlating DEGs, only *IGFBP5*[72] and *TIAM1*[73] have been previously associated with HC and/or brain growth at this age. Overall, DNAm of *DAOA, GATA4, GSDMD, INPP5D, NR2F1, RASSF4*, and *TSNARE1* and expression of *TMEM87A* correlated with HC (SD) in both at birth and at the age of six.

According to the pathway analysis (GO), the observed newborns' HC-associated genes enriched most significantly in ribosomal terms as well as in the terms of neuron to neuron synapse, postsynaptic density, and asymmetric synapse (Figure 3a, Supplementary Table S15).

Table 3. Correlations between placental PAE-associated genes and HC (SD) of the same children at birth and at the age of six. Significant correlations in DNAm and gene expression with nominal P-values <0.05 are shown in the table (Spearman). Genes previously associated with HC and/or brain growth are shown in bold, and genes correlating with HC (SD) at both ages are underlined. Correlations between newborns' HC (SD), DNAm, and gene expression were calculated using data available from the entire cohort.

HC (SD) at birth	HC (SD) at the age of six

DNAm (*n* = 174)	*ARHGEF10, CACNG7,* ***CAMTA1****, CTBP2, CTSG, CYS1, DAOA, DAPK1, DLGAP2, ERICH1, GATA4, GPHN,* ***GRIN3A****, GSDMD, H2AFY2,* ***HOXA1****_HOTAIRM1, LRRC6,* ***MYT1L****,* ***NR2F1*** *MIR548AO, OCA2,* ***PARK2****, PCDHB3, PLEKHM3,* ***PRDM16****, PRKCQ,* ***PTPRD****,* ***RAI1****, SLC12A7, SLC12A8, TSNARE1, U6, U6_CHCHD3, WASF3, ZNF256* Only PAE: *ARHGAP42, ATP11A, CLTA, CSF2, GPHN, INPP5D, ISY1_ISY1-RAB43, NRIP2_ITFG2, OSBP, PLXND1, RASSF4*	**DNAm** (*n* = 74)	*CRMP1, DAOA, DHRS2, GATA4, GSDMD,* ***GTDC1****,* ***NCAM2****, NODAL,* ***NR2F1*** *MIR548AO, PPAP2C, TSNARE1* Only PAE: *INPP5D, RASSF4*
mRNA (*n* = 109)	*AAK1, ANKRD12, AREG,* ***BCAP31****, BOD1L1, CCAR1, CLIC3, COPS9, CYP20A1, ECI1, GDPD3, GUK1, HSD3B1, INO80D, KLHL42,* ***KMT2C****, KRT18, MRPL41, NRK, OAZ1, PDCD5, PHPT1,* ***POGZ****, PPP1CA, RASAL2, ROCK1, RPL13, RPL8, RPS19BP1, RPS3,* ***RPS6****, RPS9, SERF2, SLC44A2, TBC1D5, TMC, TMEM160, TMEM87A, TPT1* Only PAE: *CORO6, GABPB1-AS1, KDM5A, LSM4, PFN1, PHLDA2, UBE2Q2*	**mRNA** (*n* = 41)	*ATP5MG, COX6A1, EFHC1, H2AC6, H2BC4, IGFBP5, MBTPS2, MRPL33, OXLD1, POLR2F, ST3GAL1,* ***TIAM1****, TMEM87A, TRIM44*

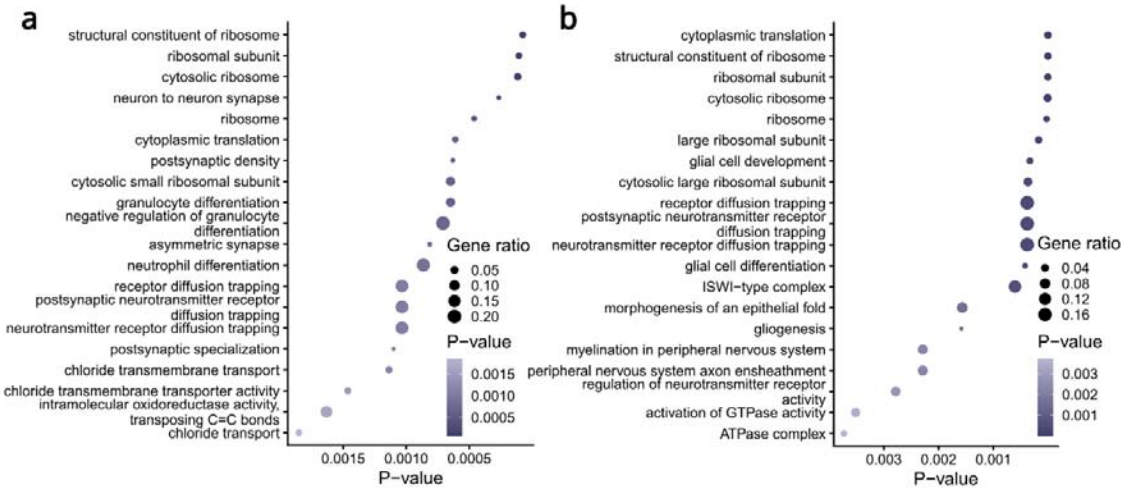

Figure 3. Enriched terms identified in GO pathway analysis of PAE-associated placental genes correlating with HC (SD) at birth and ADHD. The 20 most significant terms from GO pathway analyses of **a)** HC (SD)-correlating and **b)** ADHD-RS score-correlating genes are shown ($P<0.05$).

PAE-associated placental alterations correlated with cognitive performance scores

Several genes showed correlations between DNAm and gene expression, and cognitive performance scores ($P<0.05$, Spearman) (Table 4, Supplementary Table S13). The assessed scores included Full-Scale Intelligence Quotient (FSIQ) for overall cognitive capacity, Verbal IQ (VIQ) for verbal intellectual abilities, Performance IQ (PIQ) for nonverbal skills, Working Memory Index (WMI) for assessing ability to hold and manipulate information in short-term immediate memory, Processing Speed Quotient (PSQ) for speed and accuracy of processing, and General Language Composite (GLC) for language development[27]. Among the significantly correlated candidate genes were *DAOA (D-amino acid oxidase activator)*, which methylation of two probes correlated negatively with VIQ (r=-0.245, P=0.032 and r=-0.231, P=0.043) and GLC (r=-0.345, P=0.002 and r=-0.338, P=0.003) scores, *GPHN*, which methylation correlated negatively with WMI (r=-0.235, P=0.04), and *GLI3 (GLI family zinc finger 3)*, which expression correlated positively with WMI (r=0.37, P=0.012), analysed by Spearman. *DAOA*, which plays a modulatory role at glutamatergic synapses, has previously been associated with verbal fluency[74,75]. Additionally, *GPHN* and *GLI3* have been associated with hippocampus and memory, as well as alcohol-induced downregulation[42,76,47]. Furthermore, *CAMTA1* (correlating with PSQ)[57], *COX7B* (FSIQ, PIQ)[77], *GSDMD* (FSIQ, PIQ)[78], *LUZP1* (WMI)[79,80], *MBTPS2* (VIQ, GLC)[81], *MNX1* (VIQ, GLC)[82], *MRPL40* (PSQ)[83,84], *NDUFA4* (PIQ)[85], *NR2F1* (FSIQ, VIQ, WMI)[86], *PTRHD1* (PIQ)[87], *RAI1* (FSIQ, PIQ)[65], *RPL10* (GLC)[88], and *UFC1* (PIQ, WMI)[89] have previously been associated with cognitive impairment and/or intellectual disability. *CELF2* has been associated with cell fates in human cortical development and cognitive defects such as speech delay[90] as well as learning and memory deficits and epileptic seizures in mouse[91]. Interestingly, in this study, DNAm of *CELF2* correlated with VIQ, WMI, and GLC.

According to the pathway analysis (GO), the observed cognition-associated genes enriched most significantly in mitochondrial and ribosomal terms, such as respiratory chain complex, proton transmembrane transporter activity, and ribosomal subunit (Supplementary Table S14).

Table 4. Correlations between placental PAE-associated genes and the cognitive performances of the same children at the age of six. Significant correlations in DNAm and gene expression with *P*-values <0.05 are shown (Spearman). FSIQ: Full Scale Intelligence Quotient (IQ), VIQ: Verbal IQ, PIQ: Performance IQ, WMI: Working Memory Index, PSQ: Processing Speed Quotient, GLC: General Language Composite. Genes previously associated with impaired cognition and/or intellectual disability are shown in bold.

	FSIQ	VIQ	PIQ	WMI	PSQ	GLC
DNAm (*n* = 77)	*ERICH1, GATA4, **GSDMD**, GTSF1, H2AFY2, NODAL, **NR2F1**_MIR548AO, **RAI1**, SPRN_CYP2E1, TSNARE1, U6* Only PAE: *ARHGAP42, CLTA, TMEM133*	*ARHGEF10, **CELF2**, DAOA, DHRS2, ERICH1, FRZB, GATA4, **MNX1**, NODAL, **NR2F1**_MIR548AO, SLC12A7, SPRN_CYP2E1, TSNARE1* Only PAE: *ARHGAP42, CLTA*	*ARHGEF10, BANP, GFRA2, **GSDMD**, H2AFY2, **RAI1**, SLC12A7, SPRN_CYP2E1, SPRN_SCART1, TRIM5_OR52N1, TSNARE1, U6, U6_SLC39A14* Only PAE: *TMEM133*	***CELF2**, ERICH1, FRZB, GATA4, **GPHN**, H2AFY2, **NR2F1**_MIR548AO, PCSK9, U6, ZNF516* Only PAE: *ARHGAP42*	***CAMTA1**, CTBP2, TSNARE1, U6, U6_SLC39A14* Only PAE: *CLTA, GBP2*	*ARHGEF10, **CELF2**, DAOA, ERICH1, GATA4, **MNX1**, SLC12A8, TSNARE1, WASF3* Only PAE: *ARHGAP42, CLTA, INPP5D, NRIP2_ITFG2*
mRNA (*n* = 45)	*ATP6V1F, ATRAID, CGRRF1, CHP1, CKAP5, CLTA, **COX7B**, DAD1, GPR87, GTSF1, ITGB4, MCRIP2, MED31, MRPL52, NOP10, RPL28, RPL39, RPS3A, TMC1, TMEM160, TMEM41B, TRIM44, TWIST1*	*ATRAID, CLTA, COX5B, GPR87, GTSF1, ITGB4, **MBTPS2**, MED31, MRPL52, NDUFAB1, PSMD4, TMEM41B, TMEM87A* Only PAE: *H2AZ1, TMEM208*	*ABL2, AREG, ATP5MG, ATP5MPL, ATP6V1F, ATRAID, CGRRF1, CHP1, CKAP5, **COX7B**, DAD1, HMMR, ITGB4, MED31, **NDUFA4**, **PTRHD1**, RPL28, RPL39, RPS3A, RPS9, TMC1, TMEM160, TMEM41B,*	*ATRAID, COL6A3, COX17, COX5B, CYP20A1, DAD1, FAM43A, **GLI3**, GPR87, HMMR, ITGB4, **LUZP1**, MED31, MIF, MRPL52, MT-TV, NAA38, SMIM5, TBC1D5, TP53TG1, **UFC1**, ZFAND2A* Only PAE: *FBXO21, PTPRF, TMEM208*	*ATP6V1F, CKAP5, COX17, GLRX3, HMMR, **MRPL40**, PSG2, ROCK1, TMEM160* Only PAE: *FBXO21*	*ATL3, CTSO, ECI1, FAM43A, GPR87, GTSF1, IGSF3, INO80D, ITGB4, **MBTPS2**, MED31, MT-ND4L, PSMD4, **RPL10**, TMEM87A*

	Only PAE: *TMEM208*		*TP53TG1, TRIM44, TWIST1,* ***UFC1****, VAPA, ZFAND2A* Only PAE: *ACOT13, TMEM208*			

PAE-associated placental alterations correlated with ADHD-RS scores

Among genes that correlated with ADHD-RS scores, assessed using ADHD-RS questionnaires[27] completed by parents and teachers, several were previously associated with ADHD. These genes included *CUX1*, *ITGB4*, *NR2F1*, *PARK2*, *POGZ*, and *RAI1* in human[35], as well as hyperactivity-associated gene *ARHGEF10* in mouse[92] (Table 5, Supplementary Table S13). According to the pathway analysis (GO), the observed ADHD-associated genes enriched significantly in addition to ribosomal terms also to myelination of peripheral nervous system, activation of GTPase activity, negative regulation of neuron projection development, glial cell development, and Schwann cell development (Figure 3b, Supplementary Table S14).

Table 5. Correlations between placental PAE-associated genes and ADHD-RS scores of six-year-old PAE and control children. Significant correlations in DNAm and gene expression with *P*-values <0.01 are shown in the table (Spearman). Genes previously associated with ADHD symptoms are shown in bold.

	Inattention in ADHD-RS, parents	**Hyperactivity/impulsivity in ADHD-RS, parents**	**ADHD-RS total score, parents**
DNAm (*n* = 80)	***ARHGEF10****, CCR6, DAPK1, H2AFY2, KBTBD11,* ***NR2F1****_MIR548AO,* ***NR2F1****-AS1* Only PAE: *CLTA, GPHN, ISY1*	***ARHGEF10****, CCR6, CRB1, CTBP2, DAPK1, GTSF1, H2AFY2, KBTBD11,* ***NR2F1****_MIR548AO,* ***NR2F1****-AS1,* ***PARK2****,* ***RAI1****, SEMA6C, SULF1, TCF4, TLL1, TRIM5, TRIM5_OR52E4, TRIM5_OR52E6, TRIM5_OR52E8, U6, WASF3,*	***ARHGEF10****, CCR6, CTBP2, DAPK1, GTSF1, H2AFY2, KBTBD11,* ***NR2F1****_MIR548AO,* ***NR2F1****-AS1,* ***PARK2****,* ***RAI1****, SEMA6C, SULF1, TCF4, TLL1, TRIM5, TRIM5_OR52E4, TRIM_OR52E8, U6, WASF3, ZNF516*

		ZNF516 Only PAE: *ARHGAP42, CLTA, GPHN, ISY1, MCPH1, U6*	Only PAE: *ARHGAP42, CLTA, GPHN, ISY1, U6*
mRNA (*n* = 47)	*ATP5MD, BAZ2A, COL6A3, COX5B,* ***ITGB4****, LUZP1, RPL18A* Only PAE: *TMEM208*	*ATP5MD, BAZ2A, CLTA, COX5B, MRPL20, RPL13, RPL18A, RPS11, RPS15*	*ATP5MD, BAZ2A, CLTA, COL6A3, COX5B, DAD1, EEF1D, FKBP15,* ***ITGB4****, LUZP1, MRPL20, RPL13, RPL18A, RPLP1, RPS11, RPS15, TRAPPC2L*
	Inattention in ADHD-RS, teachers	**Hyperactivity/impulsivity in ADHD-RS, teachers**	**ADHD-RS total score, teachers**
DNAm (*n* = 64)	***ARHGEF10****, CACNG7, KBTBD11, KIAA0649, MNX1,* ***NR2F1****_MIR548AO,* ***RAI1***	***ARHGEF10****, KBTBD11,* ***RAI1***	***ARHGEF10****, CACNG7, KBTBD11, KIAA0649, MNX1,* ***NR2F1****_MIR548AO,* ***RAI1***
mRNA (*n* = 38)	*ATP6V1F, COL6A3, CRIP2, MAF, MEST, TMEM41B* Only PAE: *TMEM208*	*ATP6V1F,* ***CUX1****, EYA3,* ***POGZ****, TMEM41B, TRAPPC2L*	*ATP6V1F, COL6A3,* ***CUX1****, LAMC3,* ***POGZ****, SMIM5, TMEM41B, TRAPPC2L* Only PAE: *TMEM208*

PAE-associated placental alterations correlated with FAS dysmorphology scores

FAS dysmorphology score includes information about HC (SD), weight/height ratio, height, palpebral fissure length, as well as grades of smooth philtrum and thin vermilion[27]. Correlation analysis between PAE-associated DNAm, gene expression, and FAS dysmorphology scores of six-year-olds revealed several new candidate genes as well as already known genes involved in dysmorphology, such as *CEP152*[93], *GATA4*[94], *MEST*[95], *NR2F1*[96], *PRDM16*[97], *RAI1*[65], *RPL10*, *RPL13A*, *RPS3*[98], *SULF1*[99], and *TCF4*[100] (Table 6, Supplementary Table S13). According to the pathway analysis (GO), the observed FAS dysmorphology associated genes enriched most significantly in mitochondrial and ribosomal terms (Supplementary Table S14).

In terms of dysmorphological features, we focused specifically on midfacial hypoplasia. This feature is not included in the standard FAS facial dysmorphology scoring systems, although it is commonly associated with PAE[101]. In the correlation analysis between PAE-associated DNAm and midfacial hypoplasia scores, the most significantly correlated gene was

hypermethylated *FRZB* (*Secreted Frizzled-Related Protein 3*), an antagonist of the canonical Wnt signaling pathway, which is expressed in developing facial mesenchyme and neural crest cells, and is vital for the proper development and homeostasis of cartilage and bone[102,103] (r=0.441, P<0.001; r=0.48, P<0.001, and r=0.463, P<0.001, Spearman). The most significantly correlated gene between PAE-associated gene expression and midfacial hypoplasia scores was downregulated *TRAPPC2L*, a subunit of the TRAPP (trafficking protein particle) complex, which functions primarily in intracellular vesicular transport (r=0.639, Bonferroni P<0.001)[104]. Interestingly, also *GLI3* expression correlated negatively with both FAS dysmorphology scores (r=-0.33, P=0.033) and midfacial hypoplasia scores (r=-0.393, P=0.01) (Supplementary Table S13).

Table 6. Observed correlations between placental PAE-associated genes and FAS dysmorphology scores of six-year-old PAE and control children. Significant correlations in DNAm and gene expression with P-values <0.01 are shown (Spearman). Genes previously associated with dysmorphology are shown in bold.

	FAS dysmorphology scores
DNAm (n = 75)	*ARHGEF10, ATP2B2_MIR885, BRSK2, CACNG7, CCR6,* ***CEP152****, CRMP1, CTBP2, DAOA, DAPK1, DGKQ_IDUA_SLC26A1, DLGAP2, ERICH1, FRZB,* ***GATA4****, H2AFY2, KBTBD11, KIAA0649, KRT77, MYO7B,* ***NR2F1****_MIR548AO,* ***NR2F1****-AS1, OR52E4, OR52E6, PPP1R26,* ***PRDM16****, PRKCQ,* ***RAI1****, RASA3,* ***SULF1****, SYCN,* ***TCF4****, TMPRSS3_DSCR4-IT1, TMPRSS3_PSMG1, TRIM5, TRIM5_OR52E4, TRIM5_OR52E6, U6* Only PAE: *ARHGAP42, U6*
mRNA (n = 42)	*ACKR2, ATP6V1F, ATRAID, CHP1, CRISPLD2, DAD1, FIS1, ITGB4,* ***MEST****, MICOS13, MT-TV, NDUFS8, PSMB3,* ***RPL10****,* ***RPL13A****,* ***RPS3****, SDHB, TADA2B, TBC1D5, TMC1, TMEM127, TMEM41B, TRAPPC3, UFC1, UXT* Only PAE: *TMEM208*

DISCUSSION

To our knowledge, this is the first study to investigate the correlation between placental genome-wide DNAm and gene expression, and neuropsychological and dysmorphological characteristics of the same children. We explored the effects of PAE on placental gene regulation and found that, after excluding tobacco as a common confounder in PAE studies, a

large number of PAE-associated neuronal genes were detected in the placenta. Surprisingly many of the genes were involved in synaptic function, consistent with the prevailing consensus that alcohol exposure disrupts synaptic balance by affecting E/I transmission[14]. Our findings are consistent with the mouse study of Arzua and collagues, in which they observed numerous PAE-induced changes in synaptic and mitochondrial gene expressions, imbalance of E/I synaptic activity in brain tissue, as well as cognitive and behavioral abnormalities in offsprings[15].

PAE-associated alterations in the expression of several ribosomal and mitochondrial genes were observed. This is consistent with previous studies, since alcohol exposure has been associated with impaired ribosome biogenesis[105] as well as increased oxidative stress and mitochondrial dysfunction in several tissues[106,107], also in the rat placenta[108].

Furthermore, our findings are supported by previous studies, since same PAE-associated genes have been identified in several *in vitro* and *in vivo* studies, such as *in vitro* alcohol-exposed gastrulating cells (*ARHGEF10, IGFBP5, NODAL, PRDM16, RASA3,* as well as imprinted *DLK1*, *MEST,* and *PEG10*)[9], cortical brain organoids (*ARHGEF10, CAMTA1,* and *GRIN3A*)[109] as well as *in vivo* exposed human BECs (*ARHGEF10, ERICH1, NOS1AP, RASA3)*[110,111] human placenta *(ERICH1, DLGAP2)*[111], and mouse brain (*LAMA4*)[15].

PAE-associated DNAm and gene expression correlated with phenotypic traits at the age of six

By comparing observed molecular PAE-associated alterations in placenta and the phenotypic features of the same children at the age of six, we discovered several new candidate genes for the phenotypic features of FASD, such as *ARHGEF10, CAMTA1, CELF2, CTBP2, CTDC1, DAOA, FRZB, GABARAP, GLI3, GPHN, NR2F1, RAI1,* and *TSNARE1*. Many of the genes identified have previously been linked to syndromes and/or FASD-like features. The variants of *CAMTA1 (Calmodulin-binding transcription activator 1)* cause cerebellar dysfunction with variable cognitive and behavioral abnormalities (CECBA) characterized by intellectual disability, ataxia, hypotonia, and often microcephaly[57]. In this study, *CAMTA1* DNAm correlated with HC (SD) at birth and PSQ scores. Furthermore, disruption of *GTDC1 (GlycosylTransferase-like Domain Containing 1)* has previously been associated with NDDs, including global developmental delay, speech and language delay, intellectual disability, epilepsy, microcephaly, and developmental encephalopathy[70], and here its DNAm correlated

with HC (SD) at six years of age. *DAOA* has been linked previously to SCZ risk as well as verbal fluency[74,75,112], and currently *DAOA* DNAm correlated with language-related cognitive function (VIQ, GLC) as well as HC (SD) at birth and at six years of age, and FAS dysmorphology scores. Additionally, mutations in the nuclear receptor subfamily member gene *NR2F1* cause Bosch-Boonstra-Schaaf optic atrophy syndrome (BBSOAS) characterized by neurodevelopmental delay, ADHD, intellectual disability, ASD, and facial dysmorphology[86,96]. In this study *NR2F1* DNAm correlated with maternal alcohol consumption, HC (SD), FSIQ, VIQ, WMI, as well as ADHD-RS and FAS dysmorphology scores. Also, haploinsufficiency or mutations in *RAI1 (retinoic acid induced 1)* cause Smith–Magenis syndrome (SMS), characterized by neurobehavioral abnormalities including inattention and hyperactivity, reduced intellectual functioning, and craniofacial dysmorphology[65,113]. In this study, *RAI1* DNAm correlated with FSIQ, PIQ, as well as ADHD-RS and FAS dysmorphology scores.

Compared to DNA sequence mutations, which are mainly occurred in the genes responsible for the above-mentioned syndromes, epigenetic changes can indicate subtler alterations in gene function and therefore milder phenotypes. Conversely, studying changes in gene regulation enable to depicher developmentally important genes, many of which are rarely mutated. This highlights the benefits of an epigenetic approach.

Among the most interesting FASD candidate genes were downregulated *GLI3* and hypermethylated *GPHN*. *GLI3* is a transcription factor that mediates the Sonic hedgehog signaling pathway, which is critical for brain and craniofacial development[114]. *GLI3* is required for proper hippocampal growth and organization, a structure essential for spatial memory and learning, and its expression was downregulated by alcohol exposure during neurulation stage in previous mouse study[47,76]. Consistent with these findings, *GLI3* expression was negatively correlated with maternal alcohol consumption as well as WMI and FAS dysmorphology and midfacial hypoplasia scores of the six-year-olds in this study.

GPHN is a scaffold protein considered as a master regulator of neuronal functions, which clusters GABA alpha receptor on the postsynaptic membrane at inhibitory GABAergic and glycinergic neurons[34]. In addition to placental hypermethylated *GPHN*, we observed upregulated *GABARAP*, which binds to *GPHN* and is involved in trafficking and localization of GABA alpha receptors[115]. These changes, which have not previously been associated with

PAE, may indicate altered clustering and function of GABA alpha receptors, disrupted inhibitory synaptic function, and remodeled neuronal networks. Interestingly, altered development and reduced numbers of GABAergic interneurons have been reported in human fetal and infant brain with PAE[116] as well as a selective reduction of cerebral cortex GABA neurons in a late-gestation FASD mouse model[117]. Reduced GABA levels have been linked to diminished cognitive control and ADHD[118–120], both of which are characteristic features of the FASD phenotype[121]. Furthermore, altered *GPHN* function in the hippocampus has been linked to learning and memory deficits[122]. Consistently, in the current study, the DNAm of *GPHN* correlated with maternal alcohol consumption, WMI, and ADHD-RS scores.

Effects of PAE on developmental programming

Several of the observed PAE-associated genes function in the early embryonic patterning, such as *NODAL*, *GLI3*, *MNX1*, and imprinted *MEST*, and their DNAm or expression associated with the phenotypic features of the six-year-olds. To understand the functional context of the genes correlating with cognitive performance, ADHD-RS, and FAS dysmorphology scores more broadly, we divided the genes into functional clusters with assistance of artificial intelligence. In the case of cognitive performances, in addition to mitochondrial function, the genes are involved in the early embryonic patterning, morphogenesis, and craniofacial development, transcriptional, epigenetic, and RNA regulatory control, as well as neuronal differentiation, synaptic functions, and axon guidance (Figure 4a). In ADHD-RS scores, correlating genes are involved in early neurodevelopmental patterning and cortical regionalization, gene regulation, neuronal differentiation, cell adhesion, axon guidance, synaptic organization, and neurodevelopmental robustness (Figure 4b). Moreover, the most significantly correlated genes ($P<0.01$) in FAS dysmorphology, clustered in the functional groups of craniofacial and neural crest patterning, neurodevelopment and synaptic circuit formation, and cytoskeletal dynamics, and morphogenesis (Figure 4c). This suggests that PAE may alter gene regulation and developmental programming of the early embryo, and alterations in developmental trajectories are observable in the phenotypes of the affected children.

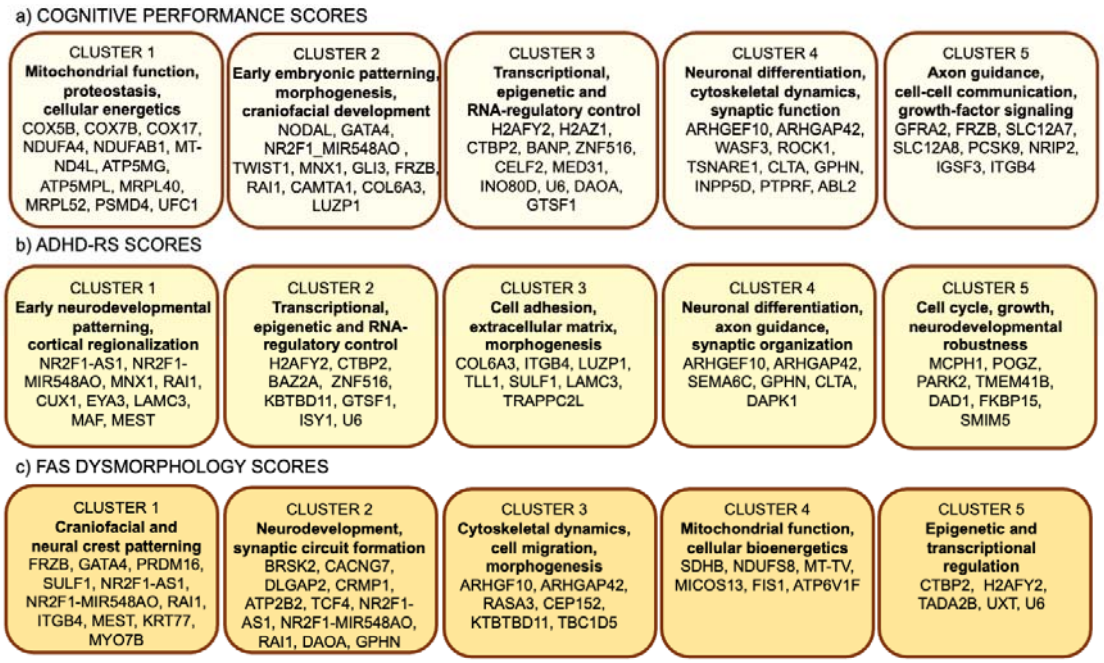

Figure 4. Functional clusters based on shared biological roles formed from placental PAE-associated genes correlating with cognitive, ADHD, and FAS dysmorphology scores of six-year-old children. Functional clusters consist of genes whose DNAm or gene expression correlated with **a)** cognitive performance, **b)** ADHD-RS, and **c)** FAS dysmorphology scores, with assistance of artificial intelligence. The clusters are in descending order according to the number of genes they contain.

Considering the high number of altered neurodevelopmental genes in the placenta, our study verifies the sensitivity of the nervous system to alcohol during developmental programming. Indeed, dysregulation of E/I balance is associated with various NDDs such as ADHD[123], ASD[124], and SCZ[125], and a large proportion of the PAE-associated genes observed in the current study have been previously associated with these disorders. Our results suggest that, despite their distinct origins, these NDDs involve shared genes and networks, resulting in partially overlapping phenotypic features[3,4]. Furthermore, since several addiction-associated genes were identified in the PAE placentas, the developmental programming of addiction should also be studied in future studies.

Placenta as a molecular window into the early development

All these changes in neurodevelopmental and synaptic genes that are observed in the placenta instead of human brain tissue emphasize the existence of a placenta-brain axis.

Although the molecular mechanisms remain poorly understood, the idea that the placenta could serve as a valuable model for elucidating human brain development and associated disorders is appealing. This perspective is supported by the alterations we observed in multiple genes involved in early embryonic development. Our findings suggest that the extraembryonic placenta—the earliest organ to form—may act as a mirror, reflecting alcohol-induced changes in gene regulation during early development across all fetal tissues, including the brain. Since alcohol exposure has been associated with alterations in the methionine cycle and DNAm[9], which play a key role in gene regulation, the role of the epigenome in the development of alcohol-induced changes is of particular interest. The persistence of PAE-induced DNAm changes across cell divisions and across different cell types and tissues would be possible through *DNA methyltransferase 1*, which maintains mitotic epigenetic memory. This is supported by similar DNAm alterations observed in previous PAE studies, as well as by the hypomethylation of the *TACR3* gene that we previously identified in the placenta, which we also observed in BECs of ectodermal origin from the newborns[19]. This possibility deserves future exploration as it could revolutionize the understanding of complex developmental disorders. Moreover, the PAE-associated changes could provide valuable biomarkers for diagnosing disorders.

Limitations

We are aware of the limitations in this study. Because the PAE-associated genes were discovered from the placenta, we do not know if the findings correspond to changes in the brain. Moreover, the causal relationship between the observed molecular alterations and neuropsychological performance at six years of age remains unknown. Furthermore, because we aimed to focus specifically on the effects of alcohol, genes influenced by both smoking and alcohol may have been excluded from the set of significant molecular changes and, consequently, from the correlation analyses. Although the molecular effects of relatively strong alcohol exposure in this cohort were detectable with the current sample size, it is insufficient for investigating genomic influences. Furthermore, we cannot rule out the influence of other prenatal confounding factors, such as maternal medications, on the placental alterations or the effects of postnatal environment on children's phenotype. Finally, information on alcohol consumption was derived mainly from maternal self-reports collected in a specialized outpatient clinic for pregnant women with substance use issues, introducing the possibility of inaccuracy.

CONCLUSION

In this study, by using an epigenetic approach and placental tissue, we bring forth PAE-induced alterations in DNAm and gene expression, which correlated with the neuropsychological and dysmorphological phenotypes of the same children at the age of six. In addition to identifying numerous candidate genes for the phenotypic features of FASD, this work highlights the placenta as a valuable model for understanding early human development and developmental disorders.

MATERIALS AND METHODS

The epiFASD cohort

Informed consent has been obtained from all participants, and we have an ethical approval (HUS/683/2020) as well as permission from Helsinki University Hospital (HUS/706/2025) for the epiFASD cohort. Women (n = 87) with substantial alcohol consumption were recruited to this study in a special outpatient clinic for pregnant women with substance use problems in Helsinki University Hospital, Finland during the years 2013–2020 (Supplementary Table S1). All newborns were children of Finnish, Caucasian mothers. The amount and timing of maternal alcohol consumption was registered using self-reported information. To avoid specific individual level data, maternal alcohol consumption is presented in three categories according to Alcohol Use Disorders Identification Test (AUDIT) scores or the number of alcohol units consumed per week (alcohol doses) (one unit is 12 g of ethyl alcohol)[126,127]. A 10-item screening tool AUDIT, developed by the World Health Organization, estimates alcohol consumption, drinking behavior, and alcohol-related problems. AUDIT scores 1–5 suggest low-risk consumption or <7 alcohol doses cause low risk for morbidity and mortality for non-pregnant women (category 1), scores 6–13 suggest hazardous or harmful alcohol consumption or 7–11 alcohol doses cause moderate risk for morbidity and mortality for non-pregnant women (category 2), and scores 14–40 indicate the likelihood of alcohol dependence (moderate-severe alcohol use disorder) or ≥12 alcohol doses cause high risk for morbidity and mortality for non-pregnant women (category 3) (Supplementary Figure S2). The timing of consumption is also presented in three categories according to the length of alcohol exposure: gestational weeks (GW) 1–12, GW 1–28, and GW 1–42. However, self-reported information (not categories) about timing of drinking,

AUDIT scores, and alcohol doses were used in statistical analyses. 18 (20.7%) of the deliveries were cesarean sections (CS). According to the medical charts, the majority, 71 (81.6%) mothers of all PAE newborns smoked, and 18 (22.5%) mothers used antidepressants or antipsychotic medication during the pregnancy. Five (6.3%) mothers used gestational diabetes mellitus medication. Four mothers had thyroid diseases, two had antihypertensive medication, and one had preventive medication for herpes. One mother had an FAS diagnosis. One mother was an occasional user of stimulants and one of cannabis. Due to the preterm premature rupture of membranes, two newborns were preterm. One of the PAE newborns had polydactyly, and three had a cleft lip.

The control samples (n = 77), collected during the years 2013–2015 in Helsinki University Hospital, Finland, were from newborns of healthy Finnish, Caucasian mothers who did not use alcohol or smoke during pregnancy according to their self-reported information (Supplementary Table S1). Five (6.5%) of the deliveries were CSs. The SEO samples (n=11), collected during the years 2013–2020 in Helsinki University Hospital, Finland, were from newborns of healthy Finnish, Caucasian mothers who smoked throughout pregnancy but did not use alcohol, according to their self-reported information (Supplementary Table S1). One (9.1%) of the deliveries was a CS.

Differences in newborn birth measures and maternal characteristics between study groups were calculated, depending on the data distribution, by Pearson's chi-square test, parametric two-tailed Student's t-test, or nonparametric Mann-Whitney U test. Differences in birth weight (BW), birth length (BL), and head circumference (HC) of the newborns were calculated using both anthropometric measures and the SDs of measures based on Finnish growth charts, in which gestational age at birth, twinning, parity, and sex were considered when calculating the SDs (z-scores) of birth measures.

Phenotypes of the epiFASD cohort children at the age of six

A total of 80 six-year-old children of the epiFASD cohort who were born in 2014-2018 participated in neuropsychological and dysmorphological assessments during 2020-2024: 28 alcohol-exposed and 52 controls. The following neuropsychological testing was performed: WPPSI-III (WPPSI-III - Wechsler Preschool and Primary Scale of Intelligence - Third Edition) and WISC-IV (Wechsler Intelligence Scale For Children – IV). ADHD-RS (ADHD Rating Scale IV) questionnaires were filled out by parents and preschool/kindergarten

teachers. Detailed dysmorphological assessments were performed. Minor anomalies and notable features were recorded and a FAS dysmorphology score was calculated based on an adaptation of Hoyme et al. (2016)[128] with minor modifications. Detailed descriptions of the tests and tested children are provided in Jolma et al. (2025)[27].

Sample collection and preparation

Placental biopsies of newborns were collected immediately after delivery. When this was not possible, placenta was stored in the fridge for a maximum of 12 h and only DNA was extracted for further analyses. Biopsies (1 cm3) were collected from the fetal side of the placenta within a radius of 2–4 cm from the umbilical cord, rinsed in cold 1× PBS, and stored in RNAlater® (Thermo Fisher Scientific) at −80 °C.

Placental genomic DNA was extracted from one to four (3.2 on average) pieces of placental tissue samples using commercial QIAamp Fast DNA Tissue or AllPrep DNA/RNA/miRNA Universal Kits (Qiagen) or standard phenol-chloroform protocol. RNA was extracted from the same placental pieces as DNA (2.9 pieces on average) by AllPrep DNA/RNA/miRNA Universal Kit. RNA quality was assessed using an Agilent 2100 Bioanalyzer (Agilent Technologies, Inc.), which was provided by the Biomedicum Functional Genomics Unit (FuGU) at the Helsinki Institute of Life Science and Biocenter Finland at the University of Helsinki.

DNAm microarrays

DNAm measurements and data processing

Genomic DNA (1000 ng) from available placental samples was sodium bisulfite-converted using the Zymo EZ DNAm™ kit (Zymo Research), and genome-wide DNAm was assessed with Infinium Methylation EPIC BeadChip Kit (Illumina) following a standard protocol at the Institute for Molecular Medicine Finland.

The raw DNAm dataset was pre-processed, quality controlled, and filtered with ChAMP R package using the minfi method[129]. Quality control was performed with the following settings: the detection *P*-value cutoff was set at $P = 0.01$, probe bead count >3 in at least 95% of samples, and the threshold for failed probes' ratio in each sample was set at 0.1. All samples passed these quality control thresholds, but 61 794 probes were excluded from the subsequent steps. Type-I and Type-II probes were normalized using the adjustedDasen

method in the wateRmelon R package[130,131]. Potential effects caused by technical factors and biological covariates were studied from singular value decomposition (SVD) plots. The data was corrected for the effects of array, slide, analysis batch, and DNA extraction method using the Empirical Bayes method implemented in ComBat function in the R package sva[132]. After ComBat adjustment, probes located in sex chromosomes and probes binding to polymorphic and off-target sites were filtered out. Also, probes in Finnish-specific single nucleotide polymorphisms (SNPs), which overlap with any known SNPs with global minor allele frequency, were removed. Population-specific masking information was obtained from Zhou et al. (2017)[133].

Subsequently, a total of 616 912 probes were retained for further downstream analysis. Annotation information was merged to corresponding probes from the IlluminaHumanMethylationEPICanno.ilm10b4.hg19 R package[134], which is based on the file "MethylationEPIC_v-1-0_B4.csv" from Illumina. Probe genomic locations relative to gene were annotated based on GENCODE Comprehensive V12 (GencodeComp) database. The following abbreviations were used: TSS1500: 1500 bp upstream of transcription start site (TSS), TSS200: 200 bp upstream of TSS, UTR: untranslated region, N_shelf: north shelf, N_shore: north shore, S_shore: south shore, S_shelf: south shelf. Probes were annotated to genes based on the University of California, Santa Cruz (UCSC) and GencodeComp databases.

The Planet R package[135] was used to estimate placental cell-type fractions in each sample by CIBERSORT method in the epiDISH R package[136]. To calculate the differences in placental cell type composition, parametric two-tailed Student's t-test or non-parametric Wilcoxon rank-sum exact tests were used. The statistical tests were selected based on assessments of data normality using the Shapiro–Wilk test and homogeneity of variances using the F-test. We observed no significant differences between the study groups in any placental cell-type.

Differentially methylated position analysis

Genome-wide differential DNAm analysis by using M-values was performed by the limma R package[137], and the linear model was adjusted based on SVD plots for technical covariates batch and DNA extraction method, biological covariates newborn sex, maternal smoking, as well as cell-type fractions. β-values were used for visualization and interpretation of the results. DMPs were considered as significant when the DNAm difference in the effect size

was ≥5% ($\Delta\beta \leq -0.05$ and $\Delta\beta \geq 0.05$) and the FDR-corrected *P*-value smaller than 0.05. Benjamini-Hochberg procedure was used to control for FDR.

Sensitivity analysis for DMPs

To test the sensitivity of DMPs, only non-smoking samples (16 PAE and 77 controls) were selected to the differential DNAm analysis, which was performed in limma and adjusted for newborn sex, batch, DNA extraction method, and cell-type fractions. Due to inflation, bacon R package was used to calculate inflation-adjusted CpGs[138]. CpGs with bacon-corrected FDR smaller than 0.05 were considered significant.

DMR analysis

The DMRcate R package was used for analysing DMRs[139]. DMRcate was set to determine probes (≥3) in a region with a maximal allowed genomic distance of 1000 bp, and scaling factor C set at 2, as per authors' recommendation. Default P-value cut-offs, including FDR<0.05 for individually significant CpGs, were used in the analysis.

Pathway analyses

Enrichment analysis was performed for PAE-associated differentially methylated CpGs (FDR<0.05) by gometh function in the missMethyl R package[140], which considers the different number of probes per gene present on the EPIC array and CpGs that are annotated to multiple genes. Enrichment analysis was also performed for PAE-associated DMRs by goregion function in missMethyl. The GO knowledgebase was used for identifying significantly enriched BP, cellular component (CC), and molecular function (MF) terms.

3'mRNA sequencing (mRNA-seq) analysis

Differential expression analysis

Extracted RNA was prepared by diluting samples to 10 ng/μl and the library preparation for bulk 3′-sequencing of poly(A)-RNA was performed as previously described[141] provided by FuGU. The libraries were sequenced on NextSeq 500 (Illumina). Drop-seq pipeline was used to construct the mRNA-seq count table for available placental RNA samples provided by FuGU. After filtering, a total of 20 851 transcripts were identified for downstream analysis. Principal component analysis implemented in the DESeq2 R package[142] was used to identify batch effects, and ComBat-seq[143] was used to adjust separate mRNA-seq batches. Differential expression analysis was performed by DESeq2, with model adjusting for smoking and

newborn sex. DEGs were considered significantly differentially expressed when FDR-corrected P-value was <0.05. Benjamini-Hochberg procedure was used to control for the FDR.

Sensitivity analysis for DEGs

To test the sensitivity of DEGs, only non-smoking samples (10 PAE and 41 controls) were selected to the differential expression analysis, which was performed in DESeq2 and adjusted for newborn sex.

Pathway analysis

enrichGO function in the clusterProfiler R package[144] were used to perform gene-set enrichment analysis for DEGs. The GO knowledgebase was used for identifying significantly enriched BP, CC, and MF terms (FDR-corrected *P*-value < 0.05). Benjamini-Hochberg procedure was used to control for FDR.

Correlations between PAE-associated genes and phenotypic features

Correlations between DMPs and significant probes (FDR < 0.05) associated with the same genes, DEGs, maternal alcohol consumption, HC (SD) at birth and at the age of six, cognitive performance, ADHD-RS scores, FAS dysmorphology scores, and midfacial hypoplasia were calculated with Spearman's rank correlation. The number of samples included in the analyses varies depending on the availability of DNAm, gene expression, and phenotype data. β-values of CpGs and vst expression counts were used. Bonferroni-adjusted significance thresholds were defined as 0.05 divided by the number of phenotypic variables multiplied by the number of DMPs or DEGs. Analyses were performed in IBM SPSS Statistics, version 30.0 (IBM Corp.).

Database comparisons

The results from DNAm and gene expression analyses were compared to various databases. Databases SZDB2.0[37] for SCZ-associated genes and SFARI Gene[36] for ASD-associated genes, as well as genes associated with ADHD according to GeneCard[35] were chosen as the conditions have partly overlapping phenotypes with FASD. MitoXplorer 3.0 web tool[32] was used to identify genes associated with mitochondrial processes. SynGO knowledgebase[33] was used to investigate the associations to synapse function.

Artificial Intelligence

Language refinement and the generation of Figure 4 were performed with assistance of artificial intelligence (ChatGPT-4.1, Perplexity, and M365 Copilot GPT-5).

ACKNOWLEDGEMENTS

We express our sincere gratitude to all the families who participated in this study. We also thank PhD Heidi Marjonen-Lindblad, as well as research nurses Teija Karkkulainen and Jaana Palukka, for their invaluable contributions.

FUNDING STATEMENT

This project was supported by The Finnish Foundation for Alcohol Studies (N.K.-A. K.R.), Research Council of Finland (grant no.: 332212, N.K.-A.), Jane and Aatos Erkko Foundation (N.K.-A.), The Foundation for Pediatric Research (N. K.-A., K.R., E.W.), Yrjö Jahnsson Foundation (N.K-A.), Liv och Hälsa Foundation (N.K-A), Instrumentarium Science Foundation (E.W.), and Märta and Peter Klaus Foundation (N.K.-A., K.R., P.A.).

REFERENCES

1. Popova, S., Lange, S., Probst, C., Gmel, G., & Rehm, J. (2017). Estimation of national, regional, and global prevalence of alcohol use during pregnancy and fetal alcohol syndrome: A systematic review and meta-analysis. *The Lancet Global Health*, *5*(3), e290–e299. https://doi.org/10.1016/S2214-109X(17)30021-9

2. Popova, S., Charness, M. E., Burd, L., Crawford, A., Hoyme, H. E., Mukherjee, R. A. S., Riley, E. P., & Elliott, E. J. (2023). Fetal alcohol spectrum disorders. *Nature Reviews Disease Primers*, *9*(1), Article 1. https://doi.org/10.1038/s41572-023-00420-x

3. Popova, S., Lange, S., Shield, K., Mihic, A., Chudley, A. E., Mukherjee, R. A. S., Bekmuradov, D., & Rehm, J. (2016). Comorbidity of fetal alcohol spectrum disorder: A systematic review and meta-analysis. *The Lancet*, *387*(10022), 978–987. https://doi.org/10.1016/S0140-6736(15)01345-8

4. Attell, B. K., Snyder, A. B., Coles, C., & Kable, J. (2025). Comorbidities associated with fetal alcohol spectrum disorders in the United States. *Scientific Reports*, *15*(1), 29704. https://doi.org/10.1038/s41598-025-13366-9

5. Owen, M. J., & O'Donovan, M. C. (2017). Schizophrenia and the neurodevelopmental continuum:evidence from genomics. *World Psychiatry*, *16*(3), 227–235. https://doi.org/10.1002/wps.20440

6. Hagan, J. F., Balachova, T., Bertrand, J., Chasnoff, I., Dang, E., Fernandez-Baca, D., Kable, J., Kosofsky, B., Senturias, Y. N., Singh, N., Sloane, M., Weitzman, C., & Zubler, J. (2016). Neurobehavioral Disorder Associated With Prenatal Alcohol Exposure. *Pediatrics*, *138*(4), e20151553. https://doi.org/10.1542/peds.2015-1553

7. Baer, J. S., Sampson, P. D., Barr, H. M., Connor, P. D., & Streissguth, A. P. (2003). A 21-Year Longitudinal Analysis of the Effects of Prenatal Alcohol Exposure on Young Adult Drinking. *Archives of General Psychiatry*, *60*(4), 377–385. https://doi.org/10.1001/archpsyc.60.4.377

8. Guerri, C. (2002). Mechanisms involved in central nervous system dysfunctions induced by prenatal ethanol exposure. *Neurotoxicity Research*, *4*(4), 327–335. https://doi.org/10.1080/1029842021000010884

9. Wallén, E., Rämö, K., Vehviläinen, J., Sokka, J., Lehtonen, M., Otonkoski, T., Trokovic, R., Auvinen, P., Kärkkäinen, O., & Kaminen-Ahola, N. (2025). Effects of alcohol on the transcriptome, methylome and metabolome of in vitro gastrulating human

embryonic cells. *Disease Models & Mechanisms*, *18*(6), dmm052150. https://doi.org/10.1242/dmm.052150

10. Wallén, E., Auvinen, P., & Kaminen-Ahola, N. (2021). The Effects of Early Prenatal Alcohol Exposure on Epigenome and Embryonic Development. *Genes*, *12*(7), Article 7. https://doi.org/10.3390/genes12071095

11. Kaminen-Ahola, N., Ahola, A., Maga, M., Mallitt, K.-A., Fahey, P., Cox, T. C., Whitelaw, E., & Chong, S. (2010). Maternal Ethanol Consumption Alters the Epigenotype and the Phenotype of Offspring in a Mouse Model. *PLOS Genetics*, *6*(1), e1000811. https://doi.org/10.1371/journal.pgen.1000811

12. Marjonen, H., Sierra, A., Nyman, A., Rogojin, V., Gröhn, O., Linden, A.-M., Hautaniemi, S., & Kaminen-Ahola, N. (2015). Early Maternal Alcohol Consumption Alters Hippocampal DNA Methylation, Gene Expression and Volume in a Mouse Model. *PLOS ONE*, *10*(5), e0124931. https://doi.org/10.1371/journal.pone.0124931

13. Wozniak, J. R., Riley, E. P., & Charness, M. E. (2019). Diagnosis, epidemiology, assessment, pathophysiology, and management of fetal alcohol spectrum disorders. *The Lancet. Neurology*, *18*(8), 760–770. https://doi.org/10.1016/S1474-4422(19)30150-4

14. Lovinger, D. M., & Roberto, M. (2025). Synaptic Effects Induced by Alcohol. *Current Topics in Behavioral Neurosciences*, *71*, 217–308. https://doi.org/10.1007/7854_2022_412

15. Arzua, T., Yan, Y., Liu, X., Dash, R. K., Liu, Q.-S., & Bai, X. (2024). Synaptic and mitochondrial mechanisms behind alcohol-induced imbalance of excitatory/inhibitory synaptic activity and associated cognitive and behavioral abnormalities. *Translational Psychiatry*, *14*, 51. https://doi.org/10.1038/s41398-024-02748-8

16. Lebel, C., Roussotte, F., & Sowell, E. R. (2011). Imaging the Impact of Prenatal Alcohol Exposure on the Structure of the Developing Human Brain. *Neuropsychology Review*, *21*(2), 102–118. https://doi.org/10.1007/s11065-011-9163-0

17. Mattson, S. N., Bernes, G. A., & Doyle, L. R. (2019). Fetal Alcohol Spectrum Disorders: A Review of the Neurobehavioral Deficits Associated With Prenatal Alcohol Exposure. *Alcoholism: Clinical and Experimental Research*, *43*(6), 1046–1062. https://doi.org/10.1111/acer.14040

18. Maltepe, E., & Fisher, S. J. (2015). Placenta: The forgotten organ. *Annual Review of Cell and Developmental Biology*, *31*, 523–552. https://doi.org/10.1146/annurev-cellbio-100814-125620

19. Auvinen, P., Vehviläinen, J., Marjonen, H., Modhukur, V., Sokka, J., Wallén, E., Rämö, K., Ahola, L., Salumets, A., Otonkoski, T., Skottman, H., Ollikainen, M., Trokovic, R., Kahila, H., & Kaminen-Ahola, N. (2022). *Chromatin remodeler developmental pluripotency associated factor 4 (DPPA4) is a candidate gene for alcohol-induced developmental disorders* (p. 2022.04.14.22273502). https://doi.org/10.1101/2022.04.14.22273502

20. Bahado-Singh, R. O., Vishweswaraiah, S., Aydas, B., & Radhakrishna, U. (2021). Placental DNA methylation changes and the early prediction of autism in full-term newborns. *PLOS ONE*, *16*(7), e0253340. https://doi.org/10.1371/journal.pone.0253340

21. Zhu, Y., Gomez, J. A., Laufer, B. I., Mordaunt, C. E., Mouat, J. S., Soto, D. C., Dennis, M. Y., Benke, K. S., Bakulski, K. M., Dou, J., Marathe, R., Jianu, J. M., Williams, L. A., Gutierrez Fugón, O. J., Walker, C. K., Ozonoff, S., Daniels, J., Grosvenor, L. P., Volk, H. E., … LaSalle, J. M. (2022). Placental methylome reveals a 22q13.33 brain

regulatory gene locus associated with autism. *Genome Biology*, *23*(1), 46. https://doi.org/10.1186/s13059-022-02613-1

22. Laufer, B. I., Neier, K., Valenzuela, A. E., Yasui, D. H., Schmidt, R. J., Lein, P. J., & LaSalle, J. M. (2022). Placenta and fetal brain share a neurodevelopmental disorder DNA methylation profile in a mouse model of prenatal PCB exposure. *Cell Reports*, *38*(9), 110442. https://doi.org/10.1016/j.celrep.2022.110442

23. Ravaei, A., Emanuele, M., Nazzaro, G., Fadiga, L., & Rubini, M. (2023). Placental DNA methylation profile as predicting marker for autism spectrum disorder (ASD). *Molecular Medicine*, *29*, 8. https://doi.org/10.1186/s10020-022-00593-3

24. Diez-Ahijado, L., Cilleros-Portet, A., Fernández-Jimenez, N., Fernández, M. F., Guxens, M., Julvez, J., Llop, S., Lopez-Espinosa, M.-J., Subiza-Pérez, M., Lozano, M., Ibarluzea, J., Sunyer, J., Bustamante, M., & Cosin-Tomas, M. (2024). Evaluating the association between placenta DNA methylation and cognitive functions in the offspring. *Translational Psychiatry*, *14*(1), 383. https://doi.org/10.1038/s41398-024-03094-5

25. Rosenfeld, C. S. (2021). The Placenta-Brain-Axis. *Journal of Neuroscience Research*, *99*(1), 271–283. https://doi.org/10.1002/jnr.24603

26. Kratimenos, P., & Penn, A. A. (2019). “Placental Programming of Neuropsychiatric Disease”. *Pediatric Research*, *86*(2), 157–164. https://doi.org/10.1038/s41390-019-0405-9

27. Jolma, M., Wallén, E., Saure, E., Rämö, K., Kahila, H., & Kaminen-Ahola, N. (2025). *Dysmorphological and neuropsychological phenotypes of prenatally alcohol-exposed six-year-old children* (p. 2025.10.28.25338948). medRxiv. https://doi.org/10.1101/2025.10.28.25338948

28. Yamazaki, T., Yang, X. O., Chung, Y., Fukunaga, A., Nurieva, R., Pappu, B., Martin-Orozco, N., Kang, H. S., Ma, L., Panopoulos, A. D., Craig, S., Watowich, S. S., Jetten, A. M., Tian, Q., & Dong, C. (2008). CCR6 Regulates the Migration of Inflammatory and Regulatory T Cells. *Journal of Immunology (Baltimore, Md.□: 1950)*, *181*(12), 8391–8401. https://doi.org/10.4049/jimmunol.181.12.8391

29. Verhoeven, K., De Jonghe, P., Van de Putte, T., Nelis, E., Zwijsen, A., Verpoorten, N., De Vriendt, E., Jacobs, A., Van Gerwen, V., Francis, A., Ceuterick, C., Huylebroeck, D., & Timmerman, V. (2003). Slowed Conduction and Thin Myelination of Peripheral Nerves Associated with Mutant Rho Guanine-Nucleotide Exchange Factor 10. *The American Journal of Human Genetics*, *73*(4), 926–932. https://doi.org/10.1086/378159

30. Plooster, M., Rossi, G., Farrell, M. S., McAfee, J. C., Bell, J. L., Ye, M., Diering, G. H., Won, H., Gupton, S. L., & Brennwald, P. (2021). Schizophrenia-Linked Protein tSNARE1 Regulates Endosomal Trafficking in Cortical Neurons. *Journal of Neuroscience*, *41*(45), 9466–9481. https://doi.org/10.1523/JNEUROSCI.0556-21.2021

31. Cheung, M. M. Y., Tsang, T. W., Watkins, R., Birman, C., Popova, S., & Elliott, E. J. (2022). Ear Abnormalities Among Children with Fetal Alcohol Spectrum Disorder: A Systematic Review and Meta-Analysis. *The Journal of Pediatrics*, *242*, 113-120.e16. https://doi.org/10.1016/j.jpeds.2021.11.016

32. Haering, M., Bondio, A. del, Puccio, H., & Habermann, B. H. (2025). mitoXplorer 3.0, A Web Tool for Exploring Mitochondrial Dynamics in Single-cell RNA-seq Data. *Journal of Molecular Biology*, *437*(15), 169004. https://doi.org/10.1016/j.jmb.2025.169004

33. Koopmans, F., van Nierop, P., Andres-Alonso, M., Byrnes, A., Cijsouw, T., Coba, M. P., Cornelisse, L. N., Farrell, R. J., Goldschmidt, H. L., Howrigan, D. P., Hussain, N. K., Imig, C., de Jong, A. P. H., Jung, H., Kohansalnodehi, M., Kramarz, B., Lipstein, N., Lovering, R. C., MacGillavry, H., … Verhage, M. (2019). SynGO: An Evidence-Based, Expert-Curated Knowledge Base for the Synapse. *Neuron*, *103*(2), 217-234.e4. https://doi.org/10.1016/j.neuron.2019.05.002

34. Tyagarajan, S. K., & Fritschy, J.-M. (2014). Gephyrin: A master regulator of neuronal function? *Nature Reviews Neuroscience*, *15*(3), 141–156. https://doi.org/10.1038/nrn3670

35. Hongyao, H., Chun, J., Xiaoyan, G., Fangfang, L., Jing, Z., Lin, Z., Pengxiang, Z., & Zengchun, L. (2023). Associative gene networks reveal novel candidates important for ADHD and dyslexia comorbidity. *BMC Medical Genomics*, *16*(1), 208. https://doi.org/10.1186/s12920-023-01502-1

36. Abrahams, B. S., Arking, D. E., Campbell, D. B., Mefford, H. C., Morrow, E. M., Weiss, L. A., Menashe, I., Wadkins, T., Banerjee-Basu, S., & Packer, A. (2013). SFARI Gene 2.0: A community-driven knowledgebase for the autism spectrum disorders (ASDs). *Molecular Autism*, *4*(1), 36. https://doi.org/10.1186/2040-2392-4-36

37. Wu, Y., Yao, Y.-G., & Luo, X.-J. (2017). SZDB: A Database for Schizophrenia Genetic Research. *Schizophrenia Bulletin*, *43*(2), 459–471. https://doi.org/10.1093/schbul/sbw102

38. Haaland, Ø. A., Romanowska, J., Gjerdevik, M., Lie, R. T., Gjessing, H. K., & Jugessur, A. (2019). A genome-wide scan of cleft lip triads identifies parent-of-origin interaction effects between ANK3 and maternal smoking, and between ARHGEF10 and alcohol consumption. *F1000Research*, *8*, 960. https://doi.org/10.12688/f1000research.19571.2

39. Özel, F., Di Criscio, M., Lupu, D. I., Sarkisyan, D., Hlady, R. A., Robertson, K. D., Bakalkin, G., Liu, Y., Biernacka, J. M., Karpyak, V. M., Ekström, T. J., & Rüegg, J. (2024). DNA methylation at *DLGAP2* and risk for relapse in alcohol dependence during acamprosate treatment. *Drug and Alcohol Dependence*, *256*, 111116. https://doi.org/10.1016/j.drugalcdep.2024.111116

40. Roland, A. V., Coelho, C. A. O., Haun, H. L., Gianessi, C. A., Lopez, M. F., D'Ambrosio, S., Machinski, S. N., Kroenke, C. D., Frankland, P. W., Becker, H. C., & Kash, T. L. (2023). Alcohol dependence modifies brain networks activated during withdrawal and reaccess: A c-fos-based analysis in mice. *Biological Psychiatry*, *94*(5), 393–404. https://doi.org/10.1016/j.biopsych.2023.01.018

41. Karpyak, V. M., Winham, S. J., Biernacka, J. M., Cunningham, J. M., Lewis, K. A., Geske, J. R., Colby, C. L., Abulseoud, O. A., Hall-Flavin, D. K., Loukianova, L. L., Schneekloth, T. D., Frye, M. A., Heit, J. A., & Mrazek, D. A. (2014). Association of GATA4 sequence variation with alcohol dependence. *Addiction Biology*, *19*(2), 312–315. https://doi.org/10.1111/j.1369-1600.2012.00482.x

42. Enoch, M.-A., Zhou, Z., Kimura, M., Mash, D. C., Yuan, Q., & Goldman, D. (2012). GABAergic gene expression in postmortem hippocampus from alcoholics and cocaine addicts; corresponding findings in alcohol-naïve P and NP rats. *PloS One*, *7*(1), e29369. https://doi.org/10.1371/journal.pone.0029369

43. Freeman, K., Staehle, M. M., Gümüş, Z. H., Vadigepalli, R., Gonye, G. E., Nichols, C. N., Ogunnaike, B. A., Hoek, J. B., & Schwaber, J. S. (2012). Rapid temporal changes in the expression of a set of neuromodulatory genes during alcohol withdrawal in the dorsal vagal complex: Molecular evidence of homeostatic disturbance. *Alcoholism, Clinical and Experimental Research*, *36*(10), 1688–1700. https://doi.org/10.1111/j.1530-0277.2012.01791.x

44. Foroud, T., Wetherill, L. F., Kramer, J., Tischfield, J. A., Nurnberger, J. I., Schuckit, M. A., Xuei, X., & Edenberg, H. J. (2008). The Tachykinin Receptor 3 Is Associated With Alcohol and Cocaine Dependence. *Alcoholism, Clinical and Experimental Research*, *32*(6), 1023–1030. https://doi.org/10.1111/j.1530-0277.2008.00663.x

45. Fonseca, T. L., Fernandes, G. W., Bocco, B. M. L. C., Keshavarzian, A., Jakate, S., Donohue, T. M., Gereben, B., & Bianco, A. C. (2019). Hepatic inactivation of the type 2 deiodinase confers resistance to alcoholic liver steatosis. *Alcoholism, Clinical and Experimental Research*, *43*(7), 1376–1383. https://doi.org/10.1111/acer.14027

46. Chen, X. D., Xiong, D. H., Yang, T. L., Pei, Y. F., Guo, Y. F., Li, J., Yang, F., Pan, F., Tan, L. J., Yan, H., Liu, X. G., Lei, S. F., Li, X., Ning, L. L., Zhu, X. Z., Levy, S., Kranzler, H. R., Farrer, L. A., Gelernter, J., … Deng, H. W. (2012). ANKRD7 and CYTL1 are novel risk genes for alcohol drinking behavior. *Chinese Medical Journal*, *125*(6), 1127–1134. https://doi.org/10.3760/cma.j.issn.0366-6999.2012.06.029

47. Boschen, K. E., Fish, E. W., & Parnell, S. E. (2021). Prenatal alcohol exposure disrupts Sonic hedgehog pathway and primary cilia genes in the mouse neural tube. *Reproductive Toxicology (Elmsford, N.Y.)*, *105*, 136–147. https://doi.org/10.1016/j.reprotox.2021.09.002

48. Zhang, D., Liu, X., Dong, X., Zhu, R., Jiang, J., Ye, Y., & Jiang, Y. (2020). Cannabinoid 1 Receptor Antagonists Play a Neuroprotective Role in Chronic Alcoholic Hippocampal Injury Related to Pyroptosis Pathway. *Alcoholism: Clinical and Experimental Research*, *44*(8), 1585–1597. https://doi.org/10.1111/acer.14391

49. Khayrullin, A., Smith, L., Mistry, D., Dukes, A., Pan, Y. A., & Hamrick, M. W. (2016). Chronic alcohol exposure induces muscle atrophy (myopathy) in zebrafish and alters the expression of microRNAs targeting the Notch pathway in skeletal muscle.

Biochemical and Biophysical Research Communications, *479*(3), 590–595. https://doi.org/10.1016/j.bbrc.2016.09.117

50. Kupfer, D. M., White, V. L., Strayer, D. L., Crouch, D. J., & Burian, D. (2013). Microarray characterization of gene expression changes in blood during acute ethanol exposure. *BMC Medical Genomics*, *6*(1), 26. https://doi.org/10.1186/1755-8794-6-26

51. Goldowitz, D., Lussier, A. A., Boyle, J. K., Wong, K., Lattimer, S. L., Dubose, C., Lu, L., Kobor, M. S., & Hamre, K. M. (2014). Molecular pathways underpinning ethanol-induced neurodegeneration. *Frontiers in Genetics*, *5*, 203. https://doi.org/10.3389/fgene.2014.00203

52. Hamada, K., Ferguson, L. B., Mayfield, R. D., Krishnan, H. R., Maienschein-Cline, M., & Lasek, A. W. (2021). Binge-Like Ethanol Drinking Activates ALK Signaling and Increases the Expression of STAT3 Target Genes in the Mouse Hippocampus and Prefrontal Cortex. *Genes, Brain, and Behavior*, e12729. https://doi.org/10.1111/gbb.12729

53. MacDonald, M., Fonseca, P. A. S., Johnson, K. R., Murray, E. M., Kember, R. L., Kranzler, H. R., Mayfield, R. D., & da Silva, D. (2024). Divergent gene expression patterns in alcohol and opioid use disorders lead to consistent alterations in functional networks within the dorsolateral prefrontal cortex. *Translational Psychiatry*, *14*, 437. https://doi.org/10.1038/s41398-024-03143-z

54. McClintick, J. N., Xuei, X., Tischfield, J. A., Goate, A., Foroud, T., Wetherill, L., Ehringer, M. A., & Edenberg, H. J. (2013). Stress-response pathways are altered in the hippocampus of chronic alcoholics. *Alcohol (Fayetteville, N.Y.)*, *47*(7), 10.1016/j.alcohol.2013.07.002. https://doi.org/10.1016/j.alcohol.2013.07.002

55. Rodd, Z. A., Kimpel, M. W., Edenberg, H. J., Bell, R. L., Strother, W. N., McClintick, J. N., Carr, L. G., Liang, T., & McBride, W. J. (2008). Differential gene expression in

the nucleus accumbens with ethanol self-administration in inbred alcohol-preferring rats. *Pharmacology, Biochemistry, and Behavior*, *89*(4), 481–498. https://doi.org/10.1016/j.pbb.2008.01.023

56. Treit, S., Zhou, D., Chudley, A. E., Andrew, G., Rasmussen, C., Nikkel, S. M., Samdup, D., Hanlon-Dearman, A., Loock, C., & Beaulieu, C. (2016). Relationships between Head Circumference, Brain Volume and Cognition in Children with Prenatal Alcohol Exposure. *PLOS ONE*, *11*(2), e0150370. https://doi.org/10.1371/journal.pone.0150370

57. Al-Kateb, H., Au, P. Y. B., Berland, S., Cogne, B., Demurger, F., Fluss, J., Isidor, B., Frank, L. M., Varvagiannis, K., Koolen, D. A., McDonald, M., Montgomery, S., Moortgat, S., Deprez, M., Karadurmus, D., Paulsen, J., Reis, A., Rieger, M., Vasileiou, G., … Shinawi, M. (2024). CAMTA1-related disorder: Phenotypic and molecular characterization of 26 new individuals and literature review. *Clinical Genetics*, *105*(3), 294–301. https://doi.org/10.1111/cge.14464

58. Boddy, A. M., Harrison, P. W., Montgomery, S. H., Caravas, J. A., Raghanti, M. A., Phillips, K. A., Mundy, N. I., & Wildman, D. E. (2017). Evidence of a Conserved Molecular Response to Selection for Increased Brain Size in Primates. *Genome Biology and Evolution*, *9*(3), 700–713. https://doi.org/10.1093/gbe/evx028

59. Conciatori, M., Stodgell, C. J., Hyman, S. L., O'Bara, M., Militerni, R., Bravaccio, C., Trillo, S., Montecchi, F., Schneider, C., Melmed, R., Elia, M., Crawford, L., Spence, S. J., Muscarella, L., Guarnieri, V., D'Agruma, L., Quattrone, A., Zelante, L., Rabinowitz, D., … Persico, A. M. (2004). Association between the *HOXA1* A218G polymorphism and increased head circumference in patients with autism. *Biological Psychiatry*, *55*(4), 413–419. https://doi.org/10.1016/j.biopsych.2003.10.005

60. Kepa, A., Martinez Medina, L., Erk, S., Srivastava, D. P., Fernandes, A., Toro, R., Lévi, S., Ruggeri, B., Fernandes, C., Degenhardt, F., Witt, S. H., Meyer-Lindenberg, A., Poncer, J.-C., Martinot, J.-L., Paillère Martinot, M.-L., Müller, C. P., Heinz, A., Walter, H., Schumann, G., & Desrivières, S. (2017). Associations of the Intellectual Disability Gene MYT1L with Helix–Loop–Helix Gene Expression, Hippocampus Volume and Hippocampus Activation During Memory Retrieval. *Neuropsychopharmacology*, *42*(13), 2516–2526. https://doi.org/10.1038/npp.2017.91

61. Bertacchi, M., Romano, A. L., Loubat, A., Tran Mau□Them, F., Willems, M., Faivre, L., Khau van Kien, P., Perrin, L., Devillard, F., Sorlin, A., Kuentz, P., Philippe, C., Garde, A., Neri, F., Di Giaimo, R., Oliviero, S., Cappello, S., D'Incerti, L., Frassoni, C., & Studer, M. (2020). NR2F1 regulates regional progenitor dynamics in the mouse neocortex and cortical gyrification in BBSOAS patients. *The EMBO Journal*, *39*(13), e104163. https://doi.org/10.15252/embj.2019104163

62. Vogelezang, S., Bradfield, J. P., Grant, S. F. A., Felix, J. F., & Jaddoe, V. W. V. (2022). Genetics of early-life head circumference and genetic correlations with neurological, psychiatric and cognitive outcomes. *BMC Medical Genomics*, *15*, 124. https://doi.org/10.1186/s12920-022-01281-1

63. Suresh, V., Bhattacharya, B., Tshuva, R. Y., Danan Gotthold, M., Olender, T., Bose, M., Pradhan, S. J., Zeev, B. B., Smith, R. S., Tole, S., Galande, S., Harwell, C. C., Baizabal, J.-M., & Reiner, O. (2024). PRDM16 co-operates with LHX2 to shape the human brain. *Oxford Open Neuroscience*, *3*, kvae001. https://doi.org/10.1093/oons/kvae001

64. Choucair, N., Mignon-Ravix, C., Cacciagli, P., Abou Ghoch, J., Fawaz, A., Mégarbané, A., Villard, L., & Chouery, E. (2015). Evidence that homozygous PTPRD gene

microdeletion causes trigonocephaly, hearing loss, and intellectual disability. *Molecular Cytogenetics*, *8*, 39. https://doi.org/10.1186/s13039-015-0149-0

65. Elsea, S. H., & Williams, S. R. (2011). Smith–Magenis syndrome: Haploinsufficiency of RAI1 results in altered gene regulation in neurological and metabolic pathways. *Expert Reviews in Molecular Medicine*, *13*, e14. https://doi.org/10.1017/S1462399411001827

66. Cacciagli, P., Sutera-Sardo, J., Borges-Correia, A., Roux, J.-C., Dorboz, I., Desvignes, J.-P., Badens, C., Delepine, M., Lathrop, M., Cau, P., Lévy, N., Girard, N., Sarda, P., Boespflug-Tanguy, O., & Villard, L. (2013). Mutations in *BCAP31* Cause a Severe X-Linked Phenotype with Deafness, Dystonia, and Central Hypomyelination and Disorganize the Golgi Apparatus. *The American Journal of Human Genetics*, *93*(3), 579–586. https://doi.org/10.1016/j.ajhg.2013.07.023

67. Rots, D., Choufani, S., Faundes, V., Dingemans, A. J. M., Joss, S., Foulds, N., Jones, E. A., Stewart, S., Vasudevan, P., Dabir, T., Park, S.-M., Jewell, R., Brown, N., Pais, L., Jacquemont, S., Jizi, K., Ravenswaaij-Arts, C. M. A. van, Kroes, H. Y., Stumpel, C. T. R. M., … Banka, S. (2024). Pathogenic variants in KMT2C result in a neurodevelopmental disorder distinct from Kleefstra and Kabuki syndromes. *American Journal of Human Genetics*, *111*(8), 1626–1642. https://doi.org/10.1016/j.ajhg.2024.06.009

68. Ye, Y., Cho, M. T., Retterer, K., Alexander, N., Ben-Omran, T., Al-Mureikhi, M., Cristian, I., Wheeler, P. G., Crain, C., Zand, D., Weinstein, V., Vernon, H. J., McClellan, R., Krishnamurthy, V., Vitazka, P., Millan, F., & Chung, W. K. (2015). De novo POGZ mutations are associated with neurodevelopmental disorders and microcephaly. *Molecular Case Studies*, *1*(1), a000455. https://doi.org/10.1101/mcs.a000455

69. Pelorosso, C., Watrin, F., Conti, V., Buhler, E., Gelot, A., Yang, X., Mei, D., McEvoy-Venneri, J., Manent, J.-B., Cetica, V., Ball, L. L., Buccoliero, A. M., Vinck, A., Barba, C., Gleeson, J. G., Guerrini, R., & Represa, A. (2019). Somatic double-hit in MTOR and RPS6 in hemimegalencephaly with intractable epilepsy. *Human Molecular Genetics*, *28*(22), 3755–3765. https://doi.org/10.1093/hmg/ddz194

70. Errichiello, E., Lecca, M., Vantaggiato, C., Motta, Z., Zanotta, N., Zucca, C., Bertuzzo, S., Piubelli, L., Pollegioni, L., & Bonaglia, M. C. (2024). Further evidence supporting the role of GTDC1 in glycine metabolism and neurodevelopmental disorders. *European Journal of Human Genetics*, *32*(8), 920–927. https://doi.org/10.1038/s41431-024-01603-0

71. Scholz, C., Steinemann, D., Mälzer, M., Roy, M., Arslan-Kirchner, M., Illig, T., Schmidtke, J., & Stuhrmann, M. (2016). *NCAM2* deletion in a boy with macrocephaly and autism: Cause, association or predisposition? *European Journal of Medical Genetics*, *59*(10), 493–498. https://doi.org/10.1016/j.ejmg.2016.08.006

72. Bobola, N., & Engist, B. (2008). IGFBP5 is a potential regulator of craniofacial skeletogenesis. *Genesis*, *46*(1), 52–59. https://doi.org/10.1002/dvg.20360

73. Yoo, S., Kim, Y., Lee, H., Park, S., & Park, S. (2012). A Gene Trap Knockout of the Tiam-1 Protein Results in Malformation of the Early Embryonic Brain. *Molecules and Cells*, *34*(1), 103–108. https://doi.org/10.1007/s10059-012-0119-x

74. Krug, A., Markov, V., Krach, S., Jansen, A., Zerres, K., Eggermann, T., Stöcker, T., Shah, N. J., Nöthen, M. M., Georgi, A., Strohmaier, J., Rietschel, M., & Kircher, T. (2011). Genetic variation in G72 correlates with brain activation in the right middle temporal gyrus in a verbal fluency task in healthy individuals. *Human Brain Mapping*, *32*(1), 118–126. https://doi.org/10.1002/hbm.21005

75. Prata, D. P., Papagni, S. A., Mechelli, A., Fu, C. H. Y., Kambeitz, J., Picchioni, M., Kane, F., Kalidindi, S., McDonald, C., Kravariti, E., Toulopoulou, T., Bramon, E., Walshe, M., Murray, R., Collier, D. A., & McGuire, P. K. (2011). Effect of d□amino acid oxidase activator (DAOA; G72) on brain function during verbal fluency. *Human Brain Mapping*, *33*(1), 143–153. https://doi.org/10.1002/hbm.21198

76. Hasenpusch-Theil, K., Magnani, D., Amaniti, E.-M., Han, L., Armstrong, D., & Theil, T. (2012). Transcriptional analysis of Gli3 mutants identifies Wnt target genes in the developing hippocampus. *Cerebral Cortex (New York, N.Y.: 1991)*, *22*(12), 2878–2893. https://doi.org/10.1093/cercor/bhr365

77. Indrieri, A., van Rahden, V. A., Tiranti, V., Morleo, M., Iaconis, D., Tammaro, R., D'Amato, I., Conte, I., Maystadt, I., Demuth, S., Zvulunov, A., Kutsche, K., Zeviani, M., & Franco, B. (2012). Mutations in COX7B Cause Microphthalmia with Linear Skin Lesions, an Unconventional Mitochondrial Disease. *American Journal of Human Genetics*, *91*(5), 942–949. https://doi.org/10.1016/j.ajhg.2012.09.016

78. Rui, W., Xiao, H., Fan, Y., Ma, Z., Xiao, M., Li, S., & Shi, J. (2021). Systemic inflammasome activation and pyroptosis associate with the progression of amnestic mild cognitive impairment and Alzheimer's disease. *Journal of Neuroinflammation*, *18*, 280. https://doi.org/10.1186/s12974-021-02329-2

79. Jordan, V. K., Zaveri, H. P., & Scott, D. A. (2015). 1p36 deletion syndrome: An update. *The Application of Clinical Genetics*, *8*, 189–200. https://doi.org/10.2147/TACG.S65698

80. Wang, X., Wang, L., Bu, Q., Xiao, Y., Zhao, Y., Jiang, L., Dai, Y., Li, H., Liu, H., Chen, Y., Flores, A. D., Zhao, Y., & Cen, X. (2025). LUZP1 Regulates Dendritic Spine Maturation and Synaptic Plasticity in the Hippocampal Dentate Gyrus of Mice. *The*

Journal of Neuroscience, *45*(20), e1867242025. https://doi.org/10.1523/JNEUROSCI.1867-24.2025

81. Oeffner, F., Fischer, G., Happle, R., König, A., Betz, R. C., Bornholdt, D., Neidel, U., del Carmen Boente, M., Redler, S., Romero-Gomez, J., Salhi, A., Vera-Casaño, Á., Weirich, C., & Grzeschik, K.-H. (2009). IFAP Syndrome Is Caused by Deficiency in MBTPS2, an Intramembrane Zinc Metalloprotease Essential for Cholesterol Homeostasis and ER Stress Response. *American Journal of Human Genetics*, *84*(4), 459–467. https://doi.org/10.1016/j.ajhg.2009.03.014

82. Cuturilo, G., Hodge, J. c., Runke, C. k., Thorland, E. c., Al-Owain, M. a., Ellison, J. w., & Babovic-Vuksanovic, D. (2016). Phenotype analysis impacts testing strategy in patients with Currarino syndrome. *Clinical Genetics*, *89*(1), 109–114. https://doi.org/10.1111/cge.12572

83. Li, J., Ryan, S. K., Deboer, E., Cook, K., Fitzgerald, S., Lachman, H. M., Wallace, D. C., Goldberg, E. M., & Anderson, S. A. (2019). Mitochondrial deficits in human iPSC-derived neurons from patients with 22q11.2 deletion syndrome and schizophrenia. *Translational Psychiatry*, *9*, 302. https://doi.org/10.1038/s41398-019-0643-y

84. Devaraju, P., Yu, J., Eddins, D., Mellado-Lagarde, M. M., Earls, L. R., Westmoreland, J. J., Quarato, G., Green, D. R., & Zakharenko, S. S. (2017). Haploinsufficiency of the 22q11.2 microdeletion gene Mrpl40 disrupts short-term synaptic plasticity and working memory through dysregulation of mitochondrial calcium. *Molecular Psychiatry*, *22*(9), 1313–1326. https://doi.org/10.1038/mp.2016.75

85. Misceo, D., Strømme, P., Bitarafan, F., Chawla, M. S., Sheng, Y., Bach de Courtade, S. M., Eide, L., & Frengen, E. (2024). Biallelic NDUFA4 Deletion Causes Mitochondrial Complex IV Deficiency in a Patient with Leigh Syndrome. *Genes*, *15*(4), 500. https://doi.org/10.3390/genes15040500

86. Bosch, D. G. M., Boonstra, F. N., Gonzaga-Jauregui, C., Xu, M., de Ligt, J., Jhangiani, S., Wiszniewski, W., Muzny, D. M., Yntema, H. G., Pfundt, R., Vissers, L. E. L. M., Spruijt, L., Blokland, E. A. W., Chen, C.-A., Lewis, R. A., Tsai, S. Y., Gibbs, R. A., Tsai, M.-J., Lupski, J. R., … Schaaf, C. P. (2014). *NR2F1* Mutations Cause Optic Atrophy with Intellectual Disability. *The American Journal of Human Genetics*, *94*(2), 303–309. https://doi.org/10.1016/j.ajhg.2014.01.002

87. Al□Kasbi, G., Al□Saegh, A., Al□Qassabi, A., Al□Jabry, T., Zadjali, F., Al□Yahyaee, S., & Al□Maawali, A. (2021). Biallelic PTRHD1 Frameshift Variants Associated with Intellectual Disability, Spasticity, and Parkinsonism. *Movement Disorders Clinical Practice*, *8*(8), 1253–1257. https://doi.org/10.1002/mdc3.13342

88. Bourque, D. K., Hartley, T., Nikkel, S. M., Pohl, D., Tétreault, M., Kernohan, K. D., & Dyment, D. A. (2018). A *de novo* mutation in *RPL10* causes a rare X-linked ribosomopathy characterized by syndromic intellectual disability and epilepsy: A new case and review of the literature. *European Journal of Medical Genetics*, *61*(2), 89–93. https://doi.org/10.1016/j.ejmg.2017.10.011

89. Nahorski, M. S., Maddirevula, S., Ishimura, R., Alsahli, S., Brady, A. F., Begemann, A., Mizushima, T., Guzmán-Vega, F. J., Obata, M., Ichimura, Y., Alsaif, H. S., Anazi, S., Ibrahim, N., Abdulwahab, F., Hashem, M., Monies, D., Abouelhoda, M., Meyer, B. F., Alfadhel, M., … Alkuraya, F. S. (2018). Biallelic UFM1 and UFC1 mutations expand the essential role of ufmylation in brain development. *Brain*, *141*(7), 1934–1945. https://doi.org/10.1093/brain/awy135

90. MacPherson, M. J., Erickson, S. L., Kopp, D., Wen, P., Aghanoori, M.-R., Kedia, S., Burns, K. M. L., Vitobello, A., Tran Mau-Them, F., Thomas, Q., Gold, N. B., Brucker, W., Amlie-Wolf, L., Gripp, K. W., Bodamer, O., Faivre, L., Muona, M., Menzies, L., Baptista, J., … Yang, G. (2021). Nucleocytoplasmic transport of the

RNA-binding protein CELF2 regulates neural stem cell fates. *Cell Reports*, *35*(10), 109226. https://doi.org/10.1016/j.celrep.2021.109226

91. Hua, M., Aghanoori, M.-R., MacPherson, M., Ren, Y., Yang, Y., Or, Y. Y., Williams, L., Gafuik, C. J., Quelin, C., Keren, B., Schuhmann, S., Vasileiou, G., Bourgois, A., Vitobello, A., Philippe, C., Stark, Z., Leventer, R. J., Tran-Mau-Them, F., Tessarech, M., … Yang, G. (2025). *Genetic variants disrupting activity-dependent CELF2 shuttling cause neuronal hyperexcitability, learning deficits, and seizures* (p. 2025.06.20.25329512). medRxiv. https://doi.org/10.1101/2025.06.20.25329512

92. Lu, D.-H., Liao, H.-M., Chen, C.-H., Tu, H.-J., Liou, H.-C., Gau, S. S.-F., & Fu, W.-M. (2018). Impairment of social behaviors in Arhgef10 knockout mice. *Molecular Autism*, *9*, 11. https://doi.org/10.1186/s13229-018-0197-5

93. Guernsey, D. L., Jiang, H., Hussin, J., Arnold, M., Bouyakdan, K., Perry, S., Babineau-Sturk, T., Beis, J., Dumas, N., Evans, S. C., Ferguson, M., Matsuoka, M., Macgillivray, C., Nightingale, M., Patry, L., Rideout, A. L., Thomas, A., Orr, A., Hoffmann, I., … Samuels, M. E. (2010). Mutations in Centrosomal Protein CEP152 in Primary Microcephaly Families Linked to MCPH4. *American Journal of Human Genetics*, *87*(1), 40–51. https://doi.org/10.1016/j.ajhg.2010.06.003

94. Garg, V., Kathiriya, I. S., Barnes, R., Schluterman, M. K., King, I. N., Butler, C. A., Rothrock, C. R., Eapen, R. S., Hirayama-Yamada, K., Joo, K., Matsuoka, R., Cohen, J. C., & Srivastava, D. (2003). GATA4 mutations cause human congenital heart defects and reveal an interaction with TBX5. *Nature*, *424*(6947), 443–447. https://doi.org/10.1038/nature01827

95. Abu-Amero, S., Monk, D., Frost, J., Preece, M., Stanier, P., & Moore, G. E. (2008). The genetic aetiology of Silver–Russell syndrome. *Journal of Medical Genetics*, *45*(4), 193–199. https://doi.org/10.1136/jmg.2007.053017

96. Rech, M. E., McCarthy, J. M., Chen, C.-A., Edmond, J. C., Shah, V. S., Bosch, D. G. M., Berry, G. T., Williams, L., Madan-Khetarpal, S., Niyazov, D., Shaw-Smith, C., Kovar, E. M., Lupo, P. J., & Schaaf, C. P. (2020). Phenotypic expansion of Bosch–Boonstra–Schaaf optic atrophy syndrome and further evidence for genotype–phenotype correlations. *American Journal of Medical Genetics Part A*, *182*(6), 1426–1437. https://doi.org/10.1002/ajmg.a.61580

97. Bjork, B. C., Turbe-Doan, A., Prysak, M., Herron, B. J., & Beier, D. R. (2010). Prdm16 is required for normal palatogenesis in mice. *Human Molecular Genetics*, *19*(5), 774–789. https://doi.org/10.1093/hmg/ddp543

98. Danilova, N., & Gazda, H. T. (2015). Ribosomopathies: How a common root can cause a tree of pathologies. *Disease Models & Mechanisms*, *8*(9), 1013–1026. https://doi.org/10.1242/dmm.020529

99. Oustah, A. A., Danesin, C., Khouri-Farah, N., Farreny, M.-A., Escalas, N., Cochard, P., Glise, B., & Soula, C. (2014). Dynamics of Sonic hedgehog signaling in the ventral spinal cord are controlled by intrinsic changes in source cells requiring Sulfatase 1. *Development*, *141*(6), 1392–1403. https://doi.org/10.1242/dev.101717

100. Amiel, J., Rio, M., Pontual, L. de, Redon, R., Malan, V., Boddaert, N., Plouin, P., Carter, N. P., Lyonnet, S., Munnich, A., & Colleaux, L. (2007). Mutations in TCF4, Encoding a Class I Basic Helix-Loop-Helix Transcription Factor, Are Responsible for Pitt-Hopkins Syndrome, a Severe Epileptic Encephalopathy Associated with Autonomic Dysfunction. *American Journal of Human Genetics*, *80*(5), 988–993. https://doi.org/10.1086/515582

101. Muggli, E., Matthews, H., Penington, A., Claes, P., O'Leary, C., Forster, D., Donath, S., Anderson, P. J., Lewis, S., Nagle, C., Craig, J. M., White, S. M., Elliott, E. J., & Halliday, J. (2017). Association Between Prenatal Alcohol Exposure and Craniofacial

Shape of Children at 12 Months of Age. *JAMA Pediatrics*, *171*(8), 771–780. https://doi.org/10.1001/jamapediatrics.2017.0778

102. Tzahor, E., Kempf, H., Mootoosamy, R. C., Poon, A. C., Abzhanov, A., Tabin, C. J., Dietrich, S., & Lassar, A. B. (2003). Antagonists of Wnt and BMP signaling promote the formation of vertebrate head muscle. *Genes & Development*, *17*(24), 3087–3099. https://doi.org/10.1101/gad.1154103

103. Lodewyckx, L., Cailotto, F., Thysen, S., Luyten, F. P., & Lories, R. J. (2012). Tight regulation of wingless-type signaling in the articular cartilage - subchondral bone biomechanical unit: Transcriptomics in Frzb-knockout mice. *Arthritis Research & Therapy*, *14*(1), R16. https://doi.org/10.1186/ar3695

104. Scrivens, P. J., Shahrzad, N., Moores, A., Morin, A., Brunet, S., & Sacher, M. (2009). TRAPPC2L is a Novel, Highly Conserved TRAPP-Interacting Protein. *Traffic*, *10*(6), 724–736. https://doi.org/10.1111/j.1600-0854.2009.00906.x

105. Flentke, G. R., Wilkie, T. E., Baulch, J., Huang, Y., & Smith, S. M. (2024). Alcohol exposure suppresses ribosome biogenesis and causes nucleolar stress in cranial neural crest cells. *PLOS ONE*, *19*(6), e0304557. https://doi.org/10.1371/journal.pone.0304557

106. Chen, J. J., Schenker, S., & Henderson, G. I. (1997). 4-hydroxynonenal levels are enhanced in fetal liver mitochondria by in utero ethanol exposure. *Hepatology (Baltimore, Md.)*, *25*(1), 142–147. https://doi.org/10.1002/hep.510250126

107. Chu, J., Tong, M., & de la Monte, S. M. (2007). Chronic ethanol exposure causes mitochondrial dysfunction and oxidative stress in immature central nervous system neurons. *Acta Neuropathologica*, *113*(6), 659–673. https://doi.org/10.1007/s00401-007-0199-4

108. Gundogan, F., Elwood, G., Mark, P., Feijoo, A., Longato, L., Tong, M., & de la Monte, S. M. (2010). Ethanol-Induced Oxidative Stress and Mitochondrial Dysfunction in Rat Placenta: Relevance to Pregnancy Loss. *Alcoholism, Clinical and Experimental Research*, *34*(3), 415–423. https://doi.org/10.1111/j.1530-0277.2009.01106.x

109. Adams, J. W., Negraes, P. D., Truong, J., Tran, T., Szeto, R. A., Guerra, B. S., Herai, R. H., Teodorof-Diedrich, C., Spector, S. A., Del Campo, M., Jones, K. L., Muotri, A. R., & Trujillo, C. A. (2023). Impact of alcohol exposure on neural development and network formation in human cortical organoids. *Molecular Psychiatry*, *28*(4), 1571–1584. https://doi.org/10.1038/s41380-022-01862-7

110. Portales-Casamar, E., Lussier, A. A., Jones, M. J., MacIsaac, J. L., Edgar, R. D., Mah, S. M., Barhdadi, A., Provost, S., Lemieux-Perreault, L.-P., Cynader, M. S., Chudley, A. E., Dubé, M.-P., Reynolds, J. N., Pavlidis, P., & Kobor, M. S. (2016). DNA methylation signature of human fetal alcohol spectrum disorder. *Epigenetics & Chromatin*, *9*, 25. https://doi.org/10.1186/s13072-016-0074-4

111. Loke, Y. J., Muggli, E., Saffery, R., Ryan, J., Lewis, S., Elliott, E. J., Halliday, J., & Craig, J. M. (2021). Sex- and Tissue-Specific Effects of Binge-Level Prenatal Alcohol Consumption on DNA Methylation at Birth. *Epigenomics*, *13*(24), 1921–1938. https://doi.org/10.2217/epi-2021-0285

112. Chen, J., Xu, Y., Zhang, J., Liu, Z., Xu, C., Zhang, K., Shen, Y., & Xu, Q. (2013). A combined study of genetic association and brain imaging on the DAOA gene in schizophrenia. *American Journal of Medical Genetics Part B: Neuropsychiatric Genetics*, *162*(2), 191–200. https://doi.org/10.1002/ajmg.b.32131

113. Linders, C. C., van Eeghen, A. M., Zinkstok, J. R., van den Boogaard, M.-J., & Boot, E. (2023). Intellectual and Behavioral Phenotypes of Smith–Magenis Syndrome:

Comparisons between Individuals with a 17p11.2 Deletion and Pathogenic RAI1 Variant. *Genes*, *14*(8), 1514. https://doi.org/10.3390/genes14081514

114. Ruiz i Altaba, A., Palma, V., & Dahmane, N. (2002). Hedgehog–GLI signaling and the growth of the brain. *Nature Reviews Neuroscience*, *3*(1), 24–33. https://doi.org/10.1038/nrn704

115. Ye, J., Zou, G., Zhu, R., Kong, C., Miao, C., Zhang, M., Li, J., Xiong, W., & Wang, C. (2021). Structural basis of GABARAP-mediated GABAA receptor trafficking and functions on GABAergic synaptic transmission. *Nature Communications*, *12*(1), 297. https://doi.org/10.1038/s41467-020-20624-z

116. Marguet, F., Friocourt, G., Brosolo, M., Sauvestre, F., Marcorelles, P., Lesueur, C., Marret, S., Gonzalez, B. J., & Laquerrière, A. (2020). Prenatal alcohol exposure is a leading cause of interneuronopathy in humans. *Acta Neuropathologica Communications*, *8*(1), 208. https://doi.org/10.1186/s40478-020-01089-z

117. Smiley, J. F., Saito, M., Bleiwas, C., Masiello, K., Ardekani, B., Guilfoyle, D. N., Gerum, S., Wilson, D. A., & Vadasz, C. (2015). Selective reduction of cerebral cortex GABA neurons in a late gestation model of fetal alcohol spectrum disorder. *Alcohol*, *49*(6), 571–580. https://doi.org/10.1016/j.alcohol.2015.04.008

118. Silveri, M. M., Sneider, J. T., Crowley, D. J., Covell, M. J., Acharya, D., Rosso, I. M., & Jensen, J. E. (2013). Frontal Lobe γ-Aminobutyric Acid Levels During Adolescence: Associations with Impulsivity and Response Inhibition. *Biological Psychiatry*, *74*(4), 296–304. https://doi.org/10.1016/j.biopsych.2013.01.033

119. Boy, F., Evans, C. J., Edden, R. A. E., Lawrence, A. D., Singh, K. D., Husain, M., & Sumner, P. (2011). Dorsolateral Prefrontal γ-Aminobutyric Acid in Men Predicts Individual Differences in Rash Impulsivity. *Biological Psychiatry*, *70*(9), 866–872. https://doi.org/10.1016/j.biopsych.2011.05.030

120. Edden, R. A. E., Crocetti, D., Zhu, H., Gilbert, D. L., & Mostofsky, S. H. (2012). Reduced GABA Concentration in Attention-Deficit/Hyperactivity Disorder. *Archives of General Psychiatry*, *69*(7), 750–753. https://doi.org/10.1001/archgenpsychiatry.2011.2280

121. Mattson, J. T., Thorne, J. C., & Kover, S. T. (2020). Relationship Between Task-Based and Parent Report-Based Measures of Attention and Executive Function in Children with Fetal Alcohol Spectrum Disorders (FASD). *Journal of Pediatric Neuropsychology*, *6*(3), 176–188. https://doi.org/10.1007/s40817-020-00089-0

122. Papadopoulos, T., Korte, M., Eulenburg, V., Kubota, H., Retiounskaia, M., Harvey, R. J., Harvey, K., O'Sullivan, G. A., Laube, B., Hülsmann, S., Geiger, J. R. P., & Betz, H. (2007). Impaired GABAergic transmission and altered hippocampal synaptic plasticity in collybistin-deficient mice. *The EMBO Journal*, *26*(17), 3888–3899. https://doi.org/10.1038/sj.emboj.7601819

123. Carter Leno, V., Begum-Ali, J., Goodwin, A., Mason, L., Pasco, G., Narvekar, N., Pickles, A., Charman, T., Johnson, M. H., & Jones, E. J. H. (2025). Cortical markers of excitation/inhibition balance are associated with sensory responsivity from infancy in longitudinal cohorts enriched for autism and ADHD. *Translational Psychiatry*, *15*(1), 532. https://doi.org/10.1038/s41398-025-03791-9

124. Rubenstein, J. L. R., & Merzenich, M. M. (2003). Model of autism: Increased ratio of excitation/inhibition in key neural systems. *Genes, Brain and Behavior*, *2*(5), 255–267. https://doi.org/10.1034/j.1601-183X.2003.00037.x

125. Liu, Y., Ouyang, P., Zheng, Y., Mi, L., Zhao, J., Ning, Y., & Guo, W. (2021). A Selective Review of the Excitatory-Inhibitory Imbalance in Schizophrenia: Underlying Biology, Genetics, Microcircuits, and Symptoms. *Frontiers in Cell and Developmental Biology*, *9*, 664535. https://doi.org/10.3389/fcell.2021.664535

126. Tynjälä, J., Kangastupa, P., Laatikainen, T., Aalto, M., & Niemelä, O. (2012). Effect of Age and Gender on the Relationship between Alcohol Consumption and Serum GGT: Time to Recalibrate Goals for Normal Ranges. *Alcohol and Alcoholism*, *47*(5), 558–562. https://doi.org/10.1093/alcalc/ags072

127. Rehm, J., Gmel, G., & Shield, K. D. (2015). *Lifetime-risk of alcohol-attributable mortality based on different levels of alcohol consumption in seven European countries: Implications for low-risk drinking guidelines*. Centre for Addiction and Mental Health. https://www.julkari.fi/handle/11111/35793

128. Hoyme, H. E., Kalberg, W. O., Elliott, A. J., Blankenship, J., Buckley, D., Marais, A.-S., Manning, M. A., Robinson, L. K., Adam, M. P., Abdul-Rahman, O., Jewett, T., Coles, C. D., Chambers, C., Jones, K. L., Adnams, C. M., Shah, P. E., Riley, E. P., Charness, M. E., Warren, K. R., & May, P. A. (2016). Updated Clinical Guidelines for Diagnosing Fetal Alcohol Spectrum Disorders. *Pediatrics*, *138*(2), e20154256. https://doi.org/10.1542/peds.2015-4256

129. Tian, Y., Morris, T. J., Webster, A. P., Yang, Z., Beck, S., Feber, A., & Teschendorff, A. E. (2017). ChAMP: Updated methylation analysis pipeline for Illumina BeadChips. *Bioinformatics*, *33*(24), 3982–3984. https://doi.org/10.1093/bioinformatics/btx513

130. Pidsley, R., Y Wong, C. C., Volta, M., Lunnon, K., Mill, J., & Schalkwyk, L. C. (2013). A data-driven approach to preprocessing Illumina 450K methylation array data. *BMC Genomics*, *14*(1), 293. https://doi.org/10.1186/1471-2164-14-293

131. Wang, Y., Gorrie-Stone, T. J., Grant, O. A., Andrayas, A. D., Zhai, X., McDonald-Maier, K. D., & Schalkwyk, L. C. (2022). InterpolatedXY: A two-step strategy to normalize DNA methylation microarray data avoiding sex bias. *Bioinformatics*, *38*(16), 3950–3957. https://doi.org/10.1093/bioinformatics/btac436

132. Leek, J. T., Johnson, W. E., Parker, H. S., Jaffe, A. E., & Storey, J. D. (2012). The sva package for removing batch effects and other unwanted variation in high-throughput experiments. *Bioinformatics*, *28*(6), 882–883. https://doi.org/10.1093/bioinformatics/bts034

133. Zhou, W., Laird, P. W., & Shen, H. (2017). Comprehensive characterization, annotation and innovative use of Infinium DNA methylation BeadChip probes. *Nucleic Acids Research*, *45*(4), e22. https://doi.org/10.1093/nar/gkw967

134. Hansen, K. D. (n.d.). *IlluminaHumanMethylationEPICanno.ilm10b4.hg19: Annotation for Illumina's EPIC methylation arrays* (Version R package version 0.6.0) [Computer software].

135. Yuan, V., Hui, D., Yin, Y., Peñaherrera, M. S., Beristain, A. G., & Robinson, W. P. (2021). Cell-specific characterization of the placental methylome. *BMC Genomics*, *22*(1), 6. https://doi.org/10.1186/s12864-020-07186-6

136. Teschendorff, A. E., Breeze, C. E., Zheng, S. C., & Beck, S. (2017). A comparison of reference-based algorithms for correcting cell-type heterogeneity in Epigenome-Wide Association Studies. *BMC Bioinformatics*, *18*, 105. https://doi.org/10.1186/s12859-017-1511-5

137. Ritchie, M. E., Phipson, B., Wu, D., Hu, Y., Law, C. W., Shi, W., & Smyth, G. K. (2015). Limma powers differential expression analyses for RNA-sequencing and microarray studies. *Nucleic Acids Research*, *43*(7), e47. https://doi.org/10.1093/nar/gkv007

138. van Iterson, M., van Zwet, E. W., Heijmans, B. T., & the BIOS Consortium. (2017). Controlling bias and inflation in epigenome- and transcriptome-wide association studies using the empirical null distribution. *Genome Biology*, *18*(1), 19. https://doi.org/10.1186/s13059-016-1131-9

139. Peters, T. J., Buckley, M. J., Statham, A. L., Pidsley, R., Samaras, K., V Lord, R., Clark, S. J., & Molloy, P. L. (2015). De novo identification of differentially methylated regions in the human genome. *Epigenetics & Chromatin*, *8*(1), 6. https://doi.org/10.1186/1756-8935-8-6

140. Phipson, B., Maksimovic, J., & Oshlack, A. (2016). missMethyl: An R package for analyzing data from Illumina's HumanMethylation450 platform. *Bioinformatics*, *32*(2), 286–288. https://doi.org/10.1093/bioinformatics/btv560

141. Macosko, E. Z., Basu, A., Satija, R., Nemesh, J., Shekhar, K., Goldman, M., Tirosh, I., Bialas, A. R., Kamitaki, N., Martersteck, E. M., Trombetta, J. J., Weitz, D. A., Sanes, J. R., Shalek, A. K., Regev, A., & McCarroll, S. A. (2015). Highly Parallel Genome-wide Expression Profiling of Individual Cells Using Nanoliter Droplets. *Cell*, *161*(5), 1202–1214. https://doi.org/10.1016/j.cell.2015.05.002

142. Love, M. I., Huber, W., & Anders, S. (2014). Moderated estimation of fold change and dispersion for RNA-seq data with DESeq2. *Genome Biology*, *15*(12), 550. https://doi.org/10.1186/s13059-014-0550-8

143. Zhang, Y., Parmigiani, G., & Johnson, W. E. (2020). ComBat-seq: Batch effect adjustment for RNA-seq count data. *NAR Genomics and Bioinformatics*, *2*(3), lqaa078. https://doi.org/10.1093/nargab/lqaa078

144. Yu, G., Wang, L.-G., Han, Y., & He, Q.-Y. (2012). clusterProfiler: An R Package for Comparing Biological Themes Among Gene Clusters. *OMICS: A Journal of Integrative Biology*, *16*(5), 284–287. https://doi.org/10.1089/omi.2011.0118